

 Open access • Posted Content • DOI:10.1101/2021.02.01.429229

Voluntary alcohol consumption disrupts coupling of prefrontal cortical activity to arousal — Source link

Grayson O. Sipe, Linares-Garcia I, Nguyen M, Elena M. Vazey ...+1 more authors

Institutions: Picower Institute for Learning and Memory, Rutgers University, University of Massachusetts Amherst

Published on: 02 Feb 2021 - bioRxiv (Cold Spring Harbor Laboratory)

Topics: Alcohol use disorder, Prefrontal cortex and Arousal

Related papers:

- [Emotional arousal and multiple memory systems in the mammalian brain](#)
- [Differential cognitive actions of norepinephrine \$\alpha_2\$ and \$\alpha_1\$ receptor signaling in the prefrontal cortex.](#)
- [The regulation of sleep and arousal: Development and psychopathology](#)
- [The prefrontal cortex, pathological anxiety, and anxiety disorders.](#)
- [Emerging role for the medial prefrontal cortex in alcohol-seeking behaviors.](#)

Share this paper:    

View more about this paper here: <https://typeset.io/papers/voluntary-alcohol-consumption-disrupts-coupling-of-hlrcipcxm>

1 **Voluntary alcohol consumption disrupts coupling of prefrontal cortical activity to arousal**

2 Grayson Sipe¹, Ivan Linares-Garcia², My Nguyen², Elena Vazey³, Rafiq Huda^{2*}

3 1. Department of Brain and Cognitive Science
4 Picower Institute for Learning and Memory
5 Massachusetts Institute of Technology, Cambridge United States

6 2. WM Keck Center for Collaborative Neuroscience
7 Department of Cell Biology and Neuroscience
8 Rutgers University – New Brunswick, Piscataway United States

9 3. Department of Biology
10 The University of Massachusetts, Amherst United States

11 *Correspondence: rafiq.huda@rutgers.edu

12 **Abstract**

13 Alcohol use disorder (AUD) exacts a major personal, societal, and economic toll. Top-down
14 control from the prefrontal cortex (PFC), a critical hub for decision making, executive, and other
15 cognitive functions, is key for the regulation of alcohol consumption. Arousal exerts profound
16 effects on cortical processing, allowing it to potentially modulate PFC functions relevant for
17 alcohol consumption and AUD. Despite this, it is unclear whether and how arousal-mediated
18 modulation of PFC circuits relates to voluntary alcohol drinking behaviors. Two-photon
19 microscopy is ideally suited for dissecting the neural circuit mechanisms underlying the effect of
20 alcohol on intact circuits in behaving animals. We addressed a major limitation of this technology
21 by developing a novel behavioral paradigm for voluntary drinking in head-fixed mice. We
22 recorded responses of layer 2/3 excitatory neurons in the anterior cingulate cortex (ACC)
23 subdivision of the PFC as mice voluntarily consumed ethanol, along with video recording of the
24 pupil to track momentary fluctuations in arousal. Ethanol consumption bidirectionally modified
25 the activity of subsets of ACC neurons, both at slow (minutes) and fast (sub-second) time scales.
26 Remarkably, we found that the coupling of arousal to ACC activity before drinking was associated
27 with subsequent ethanol engagement behavior. In turn, ethanol consumption modulated neuronal-
28 arousal coupling. Together, our results suggest neuronal-arousal coupling as a key biomarker for
29 alcohol drinking and lays the groundwork for future studies to dissect the therapeutic potential of
30 this process for AUD and other substance use disorders.

31 **Introduction**

32 Alcohol use disorder (AUD) is a debilitating set of chronic behaviors related to alcohol dependence
33 that lead to long-term health, social, and economic detriments. Behavioral paradigms in which
34 animals voluntarily self-administer ethanol are critical for understanding the molecular, cellular,
35 circuit, and systems level neuronal processes underlying alcohol-related behaviors. Binge alcohol
36 drinking is a pattern of alcohol consumption that can lead to the development of AUDs, however
37 the mechanisms that predispose binge drinkers to develop AUDs are poorly understood. Although
38 a wealth of mechanistic information has been generated by the various volitional drinking
39 paradigms¹⁻⁶, little is known about how *in vivo* neurophysiology actively changes while an animal
40 drinks alcohol.

41 The prefrontal cortex (PFC) has canonical roles in decision making, attention,
42 reward/punishment processing, social behavior, and other functions⁷⁻⁹. Consistent with the
43 association of AUD with the dysfunction of these higher-order processes¹⁰⁻¹³, the PFC is highly
44 implicated in AUD in humans¹⁴ as well as in non-human primate¹⁵ and rodent models¹⁶⁻¹⁸.
45 Significant evidence describes mechanistic changes in PFC structure and function following acute
46 or chronic ethanol exposure^{19,20}, with its effect usually assessed in separate cohorts of animals at
47 various time points throughout the exposure paradigm. Understanding how neuronal processing in
48 PFC networks on the sub-second time scale relevant for ethanol consumption behavior relates to
49 voluntary drinking and tracking this relationship across drinking is crucial for identifying the key
50 neuroadaptations that contribute to the development of AUD.

51 Many PFC-driven behaviors are modulated by internal states, including by momentary
52 fluctuations in arousal that can be approximated via changes in pupil size²¹⁻²⁵. In turn, cortical
53 activity is highly influenced by changes in arousal, with pupil dilations correlated to both increased
54 and decreased activity relative to periods of pupil constrictions²⁴⁻²⁹. The coupling of cortical
55 activity to arousal is coordinated via multiple neuromodulatory systems, such as norepinephrine²²,
56 acetylcholine²² and serotonin³⁰, as well as shifts in local inhibitory and disinhibitory circuits^{27,31,32}.
57 Ethanol exposure affects both neuromodulation^{18,33-35} and inhibition in the brain^{16,17,36-39}. Yet, the
58 relationship between voluntary ethanol consumption and the coupling between cortical activity
59 and arousal remains unexplored. Establishing this relationship is particularly important given the
60 relevance of arousal states to stress and anxiety-like phenotypes⁴⁰⁻⁴⁴ as well as neuropsychiatric

61 disorders like posttraumatic stress disorder (PTSD), which are well-established factors
62 contributing to dysfunction of the PFC⁴⁵⁻⁴⁷ and AUD^{41,48-50}.

63 Testing the effect of ethanol consumption on the activity of PFC neurons and their coupling
64 to arousal requires simultaneous measurement of neuronal activity and arousal while animals
65 voluntarily consume ethanol. Several studies have utilized behavioral paradigms in which freely
66 moving animals consume ethanol, allowing for sophisticated studies of neurophysiology during
67 drinking, including extracellular electrophysiology⁵¹⁻⁵⁴, one-photon mini-scopes⁵⁵, fiber
68 photometry⁵⁶, and optogenetics^{57,58}. To our knowledge, two-photon microscopy has not yet been
69 leveraged to investigate changes in neurophysiology during volitional ethanol consumption. Two-
70 photon microscopy complements these techniques by providing fine spatial and temporal
71 resolutions for studying the effects of ethanol on the brain. It enables analysis of population-level
72 neuronal activity at cellular resolution to study how ethanol consumption affects activity dynamics.
73 It also enables longitudinal imaging of single cells and subcellular compartments, thereby
74 providing information about the dynamics within single drinking sessions as well as over the
75 longer time scales of days and weeks. However, a key drawback of two-photon microscopy is that
76 it necessitates head-fixation for stable imaging, thereby limiting the scope of behaviors that can be
77 studied.

78 We reasoned that mice with a history of binge-like drinking would transfer their behavior
79 to drinking ethanol while being head-fixed under a two-photon microscope. We report here such
80 a paradigm to open the possibility of applying two-photon microscopy and other recording
81 modalities requiring head-fixation to the study of voluntary consumption of ethanol. In addition to
82 two-photon imaging, we also collected pupil dynamics and licking behavior to correlate changes
83 in neurophysiology in the PFC with changes in arousal and quantitative metrics of ethanol
84 drinking. We targeted the anterior cingulate cortex (ACC) subdivision of the PFC for recordings.
85 In humans, the ACC is affected by moderate doses of ethanol¹² and its structural features and
86 functional connectivity are prospectively associated with future drinking^{59,60}. Moreover, the ACC
87 is a key component of the cortical circuitry for interoceptive processing⁶¹, making it a prime
88 candidate for assessing how coupling between arousal and cortical activity relates to voluntary
89 ethanol behaviors. We find that mice consume as much or more ethanol during head-fixed drinking
90 as they do during the drinking in the dark (DID)^{1,2} paradigm in their home cages. Furthermore, we
91 find unexpected changes in neuronal activity as animals consume ethanol, especially with regards

92 to its coupling to pupil dynamics indicative of changing arousal states. These data represent the
93 first reported two-photon imaging of PFC networks while animals voluntarily consume ethanol as
94 a head-fixed extension of the DID paradigm.

95 **Results**

96 **Novel paradigm for studying voluntary ethanol consumption behavior in head-fixed mice**

97 We designed a novel behavioral paradigm for head-fixed mice to enable two-photon calcium
98 imaging during voluntary self-administration of ethanol. Mice were implanted with a head-fixation
99 bar and chronic imaging window to provide optical access for two photon microscopy in the
100 anterior cingulate cortex (ACC) subdivision of the prefrontal cortex. After recovery from surgery,
101 mice were first allowed to self-administer ethanol using the ‘drinking in the dark’ (DID)
102 paradigm^{1,2}. Mice were provided access to a bottle containing 20% ethanol in drinking water (v/v)
103 three hours into the dark phase of their light cycle for three hours every day (Fig. 1A). Mice
104 gradually increased their ethanol intake during the DID (Fig. 1B). After eight days of DID, we
105 habituated mice to head-fixation in daily sessions of 30 minutes for five days, during which mice
106 continued to undergo DID. After habituation, the DID procedure was discontinued and mice
107 instead self-administered ethanol while head-fixed under a two-photon microscope. The head-
108 fixed drinking (HFD) paradigm was performed three hours into dark phase of their light cycle, at
109 the same circadian time as the DID procedure.

110 Head-fixed mice could collect drops of a 20% ethanol solution by licking a metal spout.
111 We custom designed an electronic circuit to control ethanol delivery via a solenoid valve and to
112 measure lick responses with a capacitive sensor (Fig. S1). This circuit interfaced with custom
113 software, allowing us to control the timing and amount of ethanol delivered. Head-fixed drinking
114 sessions were organized into trials, the structure of which was not cued to the animal (Fig. 1C).
115 Each trial started with a randomized delay sampled from an exponential distribution (10s mean
116 with cutoffs at 5s and 20s). Mice triggered a drop of ethanol by licking the spout during the query
117 period (last 1s of the delay). Ethanol delivery was delayed by 1s until a lick was made during the
118 query period, thereby requiring the animal to volitionally initiate ethanol delivery via licking. The
119 un-cued trial structure and randomized delays introduced uncertainty in the ethanol delivery time,
120 potentially incentivizing licking behavior. Thus, with this self-paced contingency, mice could
121 acquire varying amounts of ethanol based on their level of engagement with drinking. Practically,
122 it also ensured that mice collected the previously dispensed drop through licking before additional
123 ethanol was delivered.

124 Mice underwent five days of HFD while being simultaneously imaged using two-photon
125 microscopy. The imaging sessions were divided into three consecutive blocks consisting of a 10
126 minute pre-drinking baseline period followed by two 10 minute drinking blocks, which we refer
127 to as early and late drinking, respectively (Fig 1A). Mice readily adapted to drinking while head-
128 fixed and consumed large amounts of ethanol in the short span of 20 minutes (4.89 ± 0.04 g/kg,
129 $n=20$ sessions, 5 days, 4 mice; Fig. 1B; Supplementary Video 1). This volume corresponded to a
130 binge-like level of blood-ethanol content (BEC; 199.3 ± 62.19 mg/dL, $n=4$ mice, final day of
131 imaging)⁶². We assessed whether mice front loaded ethanol consumption in this paradigm by
132 comparing the amount consumed during the early and late drinking blocks. Across sessions, mice
133 drank a similar amount of ethanol in each of the two drinking blocks (early: 0.39 ± 0.03 mL; late:
134 0.35 ± 0.03 mL; Fig. 1D). As mice voluntarily consumed ethanol, we measured the calcium
135 responses of layer 2/3 excitatory neurons of transgenic mice (CaMKII-Cre x Ai148D) stably
136 expressing the genetically encoded calcium sensor GCaMP6f (Fig. 1E, F). In addition, we used
137 high-speed videography to measure changes in the pupil diameter as a proxy for momentary
138 fluctuations in arousal^{26,63,64}. Together with the high-resolution readout of licking behavior, this
139 HFD paradigm allowed us to assess the effect of voluntary ethanol consumption on ACC activity
140 as well as its coupling to simultaneously measured changes in arousal (Fig. 1F).

141 **Effect of ethanol consumption on single neuron and network level activity**

142 Previous work suggests that AUD is associated with disrupted PFC processing and that ethanol
143 consumption dysregulates PFC function⁶⁵. We determined how voluntary ethanol consumption in
144 this paradigm affects neuronal activity in the ACC. While the high spatial resolution of two-photon
145 microscopy allowed us to repeatedly find the same field of views (FOVs) and longitudinally track
146 the activity of the same neurons across days of drinking (Fig. S1), in this study we prioritized
147 analysis of large populations of neurons and included responses from all recorded neurons. To
148 determine the effect of ethanol consumption on ACC activity, we detected transient increases in
149 GCaMP6f traces to quantify the frequency and amplitude of calcium events in individual neurons
150 (Fig. 2A). Inspecting the activity of single neurons across the slow time scale of the entire imaging
151 session showed diverse types of responses with drinking; while some neurons increased or
152 decreased activity, others were unaffected (Fig. 2A). To assess how the ACC population as a whole
153 responds to ethanol consumption, we compared the calcium event frequency of all recorded

154 neurons during pre-drinking and late drinking. Overall, event frequencies were largely similar
155 across these conditions (Fig. 2B). This lack of a population level effect is likely driven by
156 heterogeneity in the response profiles of individual neurons, as suggested by the single neuron
157 examples (Fig. 2A). The lack of a trial structure for the pre-drinking block makes it difficult to
158 statistically assess changes in activity levels for individual neurons in an unbiased way. We
159 addressed this issue by performing for each neuron a shuffle test which compared the observed
160 difference in activity during pre-drinking and the two drinking blocks to the difference expected
161 by chance given the overall activity in the entire recording period (see Methods). We found that
162 ethanol consumption significantly modulated the activity of a subset of neurons, increasing the
163 activity of $11.6 \pm 1.4\%$ and decreasing the activity of $13.4 \pm 1.8\%$ of neurons ($p = 0.54$, Wilcoxon
164 signed-rank test; $n = 12$ sessions from 4 mice; Fig 2C-F).

165 The above analysis considered activity changes during drinking on the timescale of
166 minutes, possibly reflecting the slow and cumulative effect of ethanol consumption throughout the
167 session. Next, we addressed how activity is modulated on the faster timescale of individual ethanol
168 delivery events. We aligned neuronal responses to the time of ethanol delivery and identified
169 modulated neurons by comparing responses before and after delivery. Similar proportions of
170 neurons had increased and decreased activity ($6.6 \pm 3.8\%$ & $4.3 \pm 3.5\%$, $p > 0.05$; Fig. 2G-I). Since
171 mice licked the metal tube to collect the ethanol drop, this activity could be related to motor
172 responses. If this were the case, we would expect that these same neurons respond to licking in
173 general. Aligning neuronal responses to the onset of licking bouts around ethanol delivery (Fig.
174 S2A) or licking during the inter-trial interval (Fig. S2B) did not show a consistent modulation in
175 activity. Hence, the observed activity modulation likely reflects the delivery and/or receipt of
176 ethanol. Together, these analyses show that ethanol delivery bidirectionally modulates ACC
177 activity both at the slow time scale of minutes and at the sub-second time scale around ethanol
178 delivery.

179 **Effect of ethanol consumption on pairwise neuronal correlations**

180 Information processing in cortical networks is critically shaped by inter-neuronal correlations
181 between pairs of neurons^{66,67}. We took advantage of the large number of simultaneously recorded
182 neurons in our dataset to test the effect of ethanol consumption on pairwise correlations. For each
183 recording session, we computed the Pearson correlation coefficient between the activity of unique

184 pairs of neurons (Fig. 2J, K). Visualizing the activity of single example pairs showed diverse
185 changes, with correlations increasing, decreasing, or being unaffected during late drinking (last 5
186 minutes of the second drinking block) as compared to pre-drinking (Fig. 2K). To examine this
187 process at the population level, we compared correlations averaged over all pairs recorded
188 simultaneously in single behavioral sessions. Ethanol consumption did not significantly affect
189 pairwise correlations (Fig. 2L). While pairwise correlations decreased as a function of distance
190 between recorded pairs of neurons, there was no difference in this relationship between pre- and
191 late drinking (Fig. S3A, B). Similarly, accounting for the average level of activity between neuron
192 pairs did not show any differences (Fig. S3C). The percentage of pairs with significant correlations
193 was similar between pre- and late drinking (Fig. S3D). Together, these analyses show that neuronal
194 correlations in the ACC are largely unaffected by ethanol consumption when considering all
195 recorded ACC neurons.

196 **Coupling between ACC activity and arousal during pre-drinking is prospectively associated** 197 **with ethanol engagement**

198 Our results thus far show that ethanol delivery modulates ACC activity. The activity of cortical
199 neurons is profoundly affected by arousal^{26,27}, which is reflected in changes in pupil size. We tested
200 whether arousal-mediated modulation of ACC activity is related to ethanol consumption. Previous
201 work shows that while activity in neurons of the posterior cortex (e.g., visual cortex) shows
202 predominantly positive correlations with the pupil (i.e., increased activity during pupil dilations),
203 frontal cortex neurons exhibit both positive and negative correlations (i.e., increased and decreased
204 activity during pupil dilations, respectively)²⁷. This suggests that subsets of frontal cortical neurons
205 are activated as others are inhibited by fluctuations in arousal. Correlating neuronal calcium traces
206 with pupil diameter during pre-drinking identified neurons with significant pupil-activity
207 correlations, with individual neurons exhibiting positive, negative, or no correlation with changes
208 in pupil diameter (Fig. 3A,B). Across the population, the pre-drinking activity of a similar
209 proportion of neurons was positively and negatively correlated with changes in pupil diameter,
210 albeit with large session-to-session variability (Fig 3C). The ability to detect activity-pupil
211 correlations could depend on the level of neuronal activity, especially for neurons with negative
212 correlations as this requires high levels of spontaneous activity when the pupil is constricted. We
213 quantified the frequency and amplitude of detected calcium events and compared these measures

214 between neurons with positive and negative correlations to pupil size. Overall, neurons correlated
215 with pupil had similar level of activity during the pre-drinking period (Fig. 3D). Thus, subsets of
216 ACC neurons have sufficient level of spontaneous activity to measure their positive and negative
217 coupling to arousal.

218 We addressed the relationship between cortical coupling to arousal during pre-drinking and
219 the level of engagement with ethanol in the subsequent drinking block. In our paradigm, mice
220 engage with ethanol by licking during the query period to trigger delivery. We defined low and
221 high engagement sessions based on the median split of triggered ethanol delivery (Fig. 3E). The
222 percentage of neurons with significant positive pupil-activity correlations during pre-drinking was
223 higher in sessions preceding high levels of ethanol engagement as compared to sessions with low
224 engagement (Fig. 3F). In contrast, the percentage of neurons with negative activity-pupil
225 correlations was similar for low and high engagement sessions (Fig. 3G). There was no difference
226 in the frequency of pre-drinking calcium activity preceding high and low sessions (Fig. 3F,G),
227 suggesting that the overall level of activity in neurons is not associated with the level of ethanol
228 engagement.

229 We further examined this phenomenon by aligning neuronal activity to the time of
230 individual pupil dilation events. To perform this analysis, we first identified individual pupil events
231 (Fig. 4A). Importantly, there were no differences in the frequency, amplitude, or duration of pupil
232 events during pre-drinking blocks preceding low and high engagement sessions (Fig. 4B). This
233 suggests that differences in pre-drinking pupil dynamics do not account for the level of subsequent
234 ethanol engagement. As expected, neurons with positive pupil-activity correlations were activated
235 as the pupil started to dilate, reaching maximal activity before the peak of pupil dilation;
236 meanwhile, neurons negatively coupled to arousal had decreased activity during pupil dilations
237 (Fig. 4C). Importantly, neurons with positive pupil-activity correlations had increased pupil-
238 aligned responses preceding high as compared to low engagement sessions (Fig. 4C, D). In
239 contrast, the pupil aligned activity of negatively correlated neurons was similar for both sessions
240 (Fig. 4C, E).

241 Thus far, we have focused on neurons that show significant pupil-activity correlations. We
242 next assessed overall neuronal-arousal coupling in the ACC population by analyzing the pupil
243 aligned responses of all neurons. As expected, combining neurons with both positive and negative
244 pupil correlations as well as uncoupled neurons showed less arousal modulation than observed

245 before (Fig 4F). Despite this, activity around pupil dilation events was higher during pre-drinking
246 blocks preceding high engagement sessions as compared to low sessions (Fig. 4G). Together, we
247 find that the level of positive coupling between ACC activity and pupil-linked arousal during pre-
248 drinking is prospectively associated with subsequent engagement with ethanol. Importantly, this
249 association is not explained by differences in pre-drinking pupil dynamics (Fig. 4B). Rather, it
250 reflects the effect of arousal on cortical circuits, predominantly on neurons that are activated by
251 arousal (Fig. 4C, D, F, G).

252 **Ethanol consumption reconfigures the coupling between arousal and neuronal activity**

253 The above results establish neuronal-arousal coupling as an important factor for ethanol related
254 behavior in this paradigm. We determined how ethanol consumption affects this coupling. Our
255 previous analysis (Figs. 3, 4) only examined neuronal-arousal coupling during the pre-drinking
256 period, leaving open the possibility that additional neurons in the population become coupled to
257 arousal with drinking. Hence, we identified arousal modulated neurons as ones with significant
258 pupil-activity correlations either during pre-drinking or the subsequent drinking blocks. Across the
259 population, a similar proportion of neurons had positive or negative coupling to arousal (positive:
260 $55\pm 5.2\%$; negative: $45.5\pm 5.6\%$; $p = 0.14$, two-sided Wilcoxon rank-sum test; $n = 12$ behavioral
261 sessions from 4 mice). To track the evolution of neuronal-arousal coupling during the entire
262 imaging session, we computed pupil-activity correlation coefficients in five-minute bins across
263 drinking (Fig 5A). For cells with positive coupling, drinking had no significant effect on pupil-
264 activity correlations (Fig. 5A, B). In contrast, drinking decreased negative coupling to arousal (Fig.
265 5D, E). Importantly, the frequency of calcium events for both positively and negatively coupled
266 neurons were unaffected by drinking (Fig. 5C, F), suggesting that the observed changes in coupling
267 to arousal are not due to gross changes in neuronal activity.

268 We investigated which factors contribute to the observed changes in pupil-activity
269 correlations with ethanol consumption. Drinking had moderate effects on the pupil dynamics,
270 leading to a non-significant decrease in the pupil event frequency and increase in event duration
271 (Fig. S4). A change in the frequency of pupil fluctuations without a concomitant change in the
272 frequency of neuronal activity could in principle account for the observed decrease in pupil-
273 activity correlations. We controlled for this by analyzing pupil-aligned neuronal responses. The
274 pupil-aligned responses of positively coupled neurons were increased in late drinking compared

275 to pre-drinking, largely mirroring the broadening of pupil dilation events observed with drinking
276 (Fig. 5G). In contrast, the activity of negatively coupled neurons exhibited less arousal-mediated
277 modulation with drinking, showing a reduction in decreased activity observed around pupil
278 dilation events compared to pre-drinking (Fig. 5H). These results suggest that ethanol consumption
279 shifts the balance of neuronal-arousal responses to favor excitatory coupling. In agreement, pupil-
280 aligned activity of all ACC neurons analyzed without regard to their coupling to arousal showed
281 increased activity with drinking as compared to pre-drinking (Fig. 5I). Together, these results
282 demonstrate that ethanol consumption asymmetrically reconfigures the coupling between arousal
283 and neuronal activity, weakening negative and strengthening positive neuronal-arousal coupling.

284 **Discussion**

285 We developed a novel behavioral paradigm for voluntary ethanol consumption in head-fixed mice
286 (Fig. 1). This allowed the application of two-photon microscopy to measure diverse facets of
287 neuronal signaling in the ACC, components of which were prospectively associated with ethanol
288 engagement in addition to being affected by drinking. Freely moving mice readily transitioned
289 from the DID paradigm to consuming ethanol while head-fixed (Fig. 1A-C). Measuring neuronal
290 activity in layer 2/3 excitatory neurons of the ACC showed that ethanol self-administration
291 modulates neuronal activity, both at the sub-second time scale during consumption of individual
292 drops of ethanol and at the slower time scale of minutes throughout drinking (Fig. 2). Interestingly,
293 there was a bidirectional relationship between ethanol consumption and neuronal-arousal
294 coupling. Increased neuronal excitation in response to arousal during pre-drinking was
295 prospectively associated with higher levels of ethanol engagement (Figs. 3, 4). Importantly, pupil
296 dynamics were similar preceding high and low ethanol engagement sessions; hence, this coupling
297 effect is due to cortical responses to arousal rather than the level of arousal itself. In parallel,
298 drinking shifted the balance of neuronal-arousal coupling, weakening inhibitory and strengthening
299 excitatory responses to arousal (Fig. 5). Although small subsets of ACC neurons did show activity
300 modulation with drinking, the observed changes in neuronal-arousal coupling were not
301 accompanied by changes in the overall activity level of neurons. This demonstrates that for most
302 ACC neurons, ethanol consumption largely exerts a selective effect on responses to momentary
303 fluctuations in internal state shifts rather than a non-specific effect on their activity. Together, the
304 fact that ethanol increased excitatory responses to arousal and that increased responses to arousal

305 before drinking are prospectively associated with high ethanol engagement suggests ethanol-
306 mediated reconfiguration of neuronal-arousal coupling as an important signature of
307 neuroadaptations relevant for AUD.

308 The extension of the DID paradigm to head-fixed drinking allows the application of two-
309 photon microscopy to the study of voluntary ethanol-related behaviors. The high spatial resolution
310 of two-photon imaging allows longitudinal tracking of physiological adaptations simultaneously
311 with ethanol engagement (Fig. S1B). While longitudinal experiments with cellular-resolution have
312 been performed with one-photon microendoscopy in freely moving animals⁵⁵, the GRIN lenses
313 required for this technique have a limited depth of imaging compared to two-photon imaging
314 through chronic windows. Moreover, a key advantage of using head-fixation is the ability to collect
315 precise behavioral measures of ethanol consumption including simultaneous high-speed
316 acquisition of pupil dynamics, locomotion, lick microstructure, whisking, and limb kinetics^{68,69}.
317 Combination of two-photon imaging with specific transgenic mouse lines^{70,71} and viral vectors for
318 projection-specific labeling⁷², along with the expanding gamut of optical sensors for measuring
319 neuronal activity as well as extracellular release of neurotransmitters⁷³, will allow future
320 experiments to study the effect of voluntary ethanol consumption on processing by cell-specific
321 circuits. Indeed, two-photon imaging was recently used to examine changes in cortical visual
322 processing in anesthetized mice that had previously undergone chronic exposure to ethanol⁷⁴.
323 Similarly, two-photon calcium imaging is beginning to identify how systemically injected ethanol
324 modulates neuromodulator release and non-neuronal cell types⁷⁵.

325 The head-fixation required for two-photon imaging poses limitations. Recent work shows
326 that head-fixation in mice initially increases levels of the stress-related hormone corticosterone,
327 which normalizes over days with habituation⁷⁶. We previously measured circulating corticosterone
328 levels under head fixation relative to other stressors. While habituated head-fixation elicits
329 significantly less stress hormone release compared to restraint stress paradigms, it is still
330 significantly elevated from baseline in naïve mice⁷⁷. Another limitation is the temporal resolution
331 of measured neuronal activity using two-photon microscopy. Calcium-based neuronal activity
332 profiles are orders of magnitude slower than electrophysiological techniques, though our head-
333 fixed approach can be used with emerging tools for voltage imaging or high-density
334 electrophysiology such as NeuroPixel probes⁷⁸ that also require head-fixation. Given these

335 limitations, two-photon microscopy is a complementary approach to electrophysiological studies
336 in freely-moving paradigms with specific unique advantages.

337 While we used the head-fixed drinking paradigm to study various aspects of activity in the
338 ACC and volitional ethanol consumption, we envision our approach as a baseline head-fixed
339 paradigm that can be easily modified to address other important questions relevant for AUD,
340 including stress-ethanol interactions⁷⁹ and instrumental ethanol seeking⁸⁰. We found that mice
341 consumed large quantities of ethanol during head-fixed drinking. Given the well-appreciated
342 relationship between stress and excessive drinking in humans and in animal models^{48,81,82}, one
343 possibility is that the mild stress associated with head-fixation promotes drinking in this paradigm.
344 Hence, this paradigm, combined with other stressors, can be leveraged to dissect the relationship
345 between ethanol consumption and stress as well as the neuronal-arousal coupling described here.
346 This paradigm may also facilitate the study of compulsive ethanol-related behaviors^{51,83,84} in head-
347 fixed mice. Here, drops of ethanol were available after random delays drawn from an exponential
348 distribution. Such delays have a flat subjective hazard rate and disallow subjects from predicting
349 when an event will occur^{85,86}. In this regard, our paradigm is similar to conditioning experiments
350 using random interval reinforcement schedules, which are thought to promote compulsive
351 behavior⁸⁷. This suggests that the high levels of drinking observed in our model may be extended
352 to investigate punishment-resistant compulsive drinking, at least in a subset of mice. Future
353 modifications that allow testing this and other AUD-related behaviors in head-fixed mice will
354 allow application of two-photon microscopy to these questions.

355 We found that voluntary ethanol consumption in awake mice both increased and decreased
356 the activity of subpopulations of ACC neurons at the slow time scale of minutes as well as on the
357 faster time scale of individual ethanol delivery events (Fig. 2). In anesthetized rats, intraperitoneal
358 injection of ethanol dose-dependently inhibited the activity of PFC neurons recorded via
359 extracellular electrophysiology⁸⁸. Subsequent work directly compared the effect of ethanol
360 injections in anesthetized vs. awake conditions and found decreased activity during anesthesia but
361 generally no overall changes in activity levels during wakefulness⁸⁹. This suggests that ethanol has
362 a particularly depressive effect on PFC activity in the anesthetized state. Compared to systemic
363 ethanol injections, voluntary ethanol consumption may induce more heterogenous activity patterns
364 that potentially reflect multiple processes including the intent to drink, olfaction,
365 gustatory/consummatory responses, olfaction, and others. Future adaptations in the behavioral

366 paradigm that carefully distinguish between these processes are needed to clarify the precise nature
367 of this observed activity.

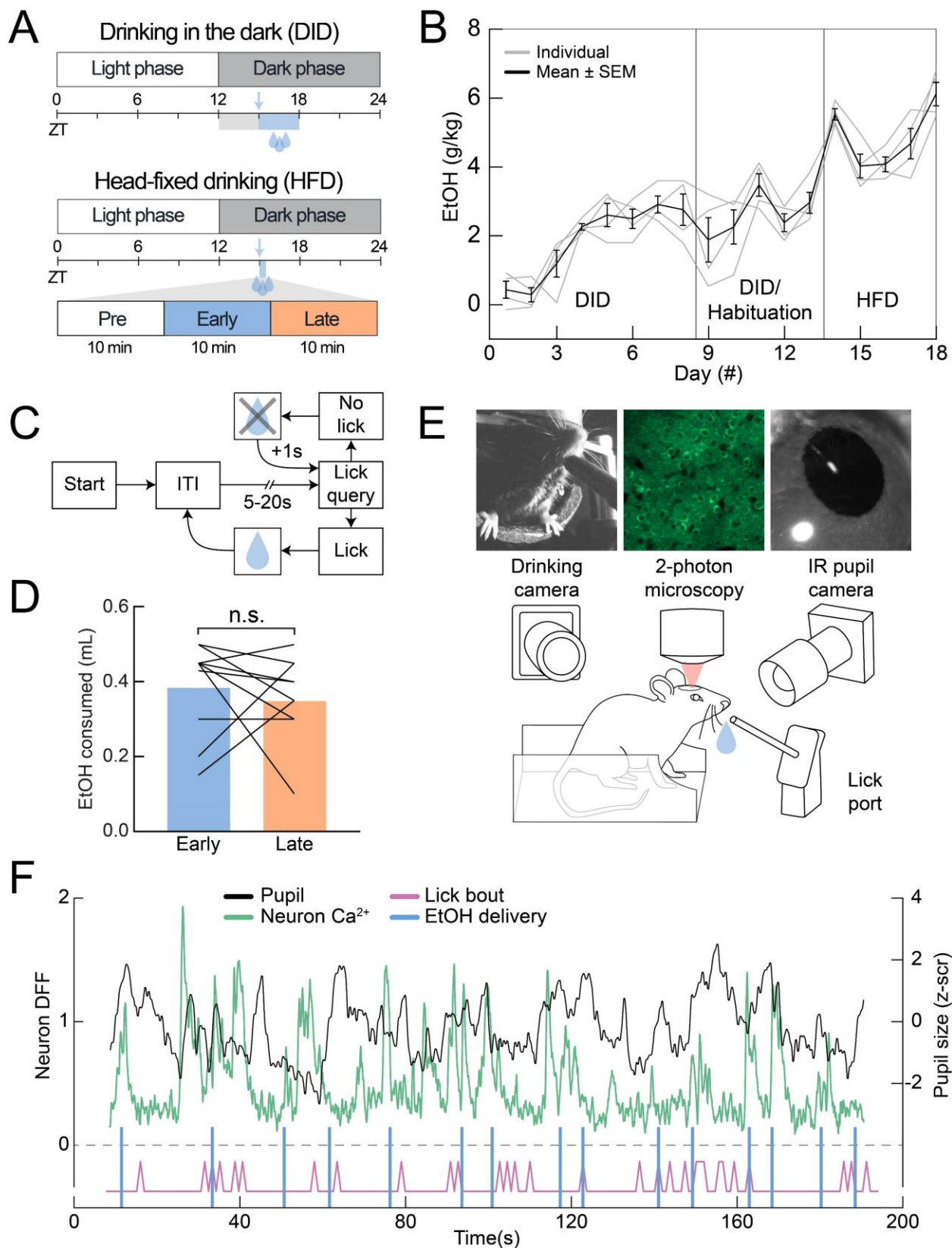
368 We focused on the activity of layer 2/3 excitatory neurons, however the observed coupling
369 of neuronal activity to the pupil suggests involvement of inhibition. Processing in cortical circuits
370 is crucially coordinated by precise spatiotemporal inhibition, with recent studies highlighting the
371 role of molecularly defined inhibitory neurons in neuronal-arousal coupling^{70,90,91}. Vasointestinal
372 peptide (VIP) expressing interneurons provide inhibition onto other inhibitory neurons, including
373 the somatostatin (SOM) expressing subtype^{32,92-94}. Activation of pyramidal neurons during arousal
374 is thought to reflect a disinhibitory microcircuit motif wherein arousal-mediated activation of VIP
375 cells causes inhibition of SOM cells and disinhibition of pyramidal neurons, thereby providing a
376 potential mechanism for positive responses to arousal. In the frontal cortex, direct VIP inhibitory
377 inputs onto pyramidal cells are proposed to mediate the negative responses to arousal²⁷. Thus, one
378 possibility is that ethanol exposure reconfigures neuronal-arousal coupling by reshaping these
379 inhibitory circuits and shifting the balance between inhibition and disinhibition of pyramidal
380 neurons. Alterations in inhibition are commonly found in response to ethanol exposure, with the
381 general finding that inhibition is reduced^{95,96}. Importantly, recent work has started addressing how
382 specific subtypes of cortical interneurons are affected, uncovering changes in SOM neuron
383 intrinsic excitability and synaptic outputs that could be particularly relevant for neuronal-arousal
384 coupling^{97,98}.

385 In addition to altered inhibition, cortical brain state shifts are strongly correlated with brain-
386 wide release of neuromodulators including norepinephrine, acetylcholine, corticosterone, and
387 serotonin^{22,24,28,30}. Numerous studies have implicated dysregulated neuromodulatory activity with
388 AUDs, suggesting that neuronal coupling to arousal may be a signature of neuromodulation
389 indicative of drinking behaviors^{33,49,99}. Relatedly, acute exposure to ethanol profoundly disrupts
390 the activity of locus coeruleus noradrenergic neurons^{75,100}, which form a key component of the
391 brain's neuromodulatory arousal system¹⁰¹. Future work will be needed to address the causal
392 relationship between neuromodulatory systems, arousal-coupled cortical activity, and ethanol
393 consumption.

394 Although considerable mechanistic research has been done on the acute cellular effects of
395 ethanol, including effects on the fast time scales of ion channel activity and synaptic
396 transmission¹⁰²⁻¹⁰⁷, as well as the chronic long-term circuit neuroadaptations^{36,108-110}, relatively few

397 studies have studied changes in the intervening time course of cortical information processing. Our
398 work bridges these timescales by focusing on how acute ethanol engagement modifies circuit
399 dynamics on the order of internal state shifts, which are highly relevant for behavioral functions
400 often associated with the PFC. Better understanding the effect of ethanol on this intermediate
401 timescale will further clarify the relationship between the myriad of behavioral and neuronal
402 adaptations that comprise AUD.

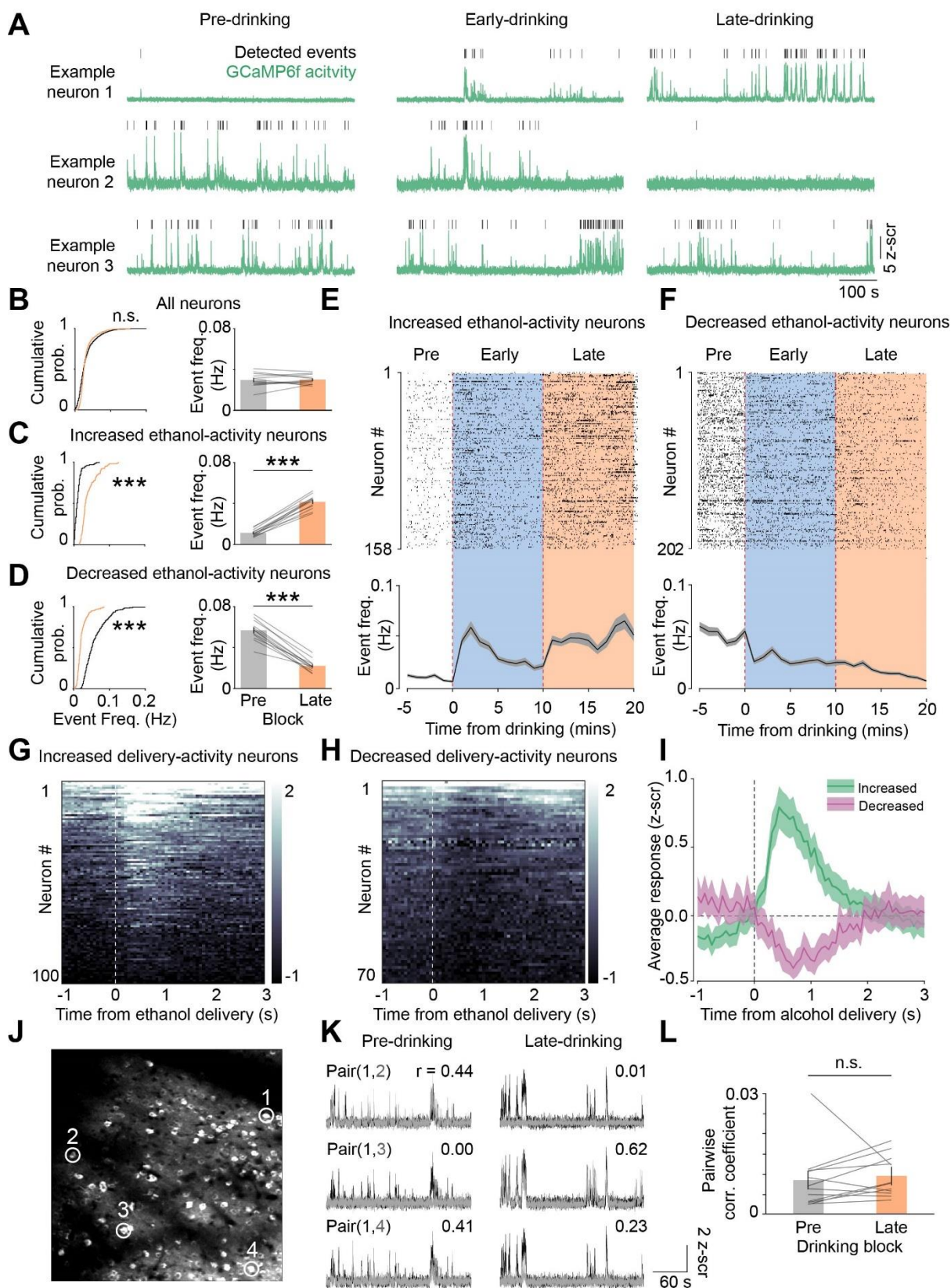
403 **Figures**



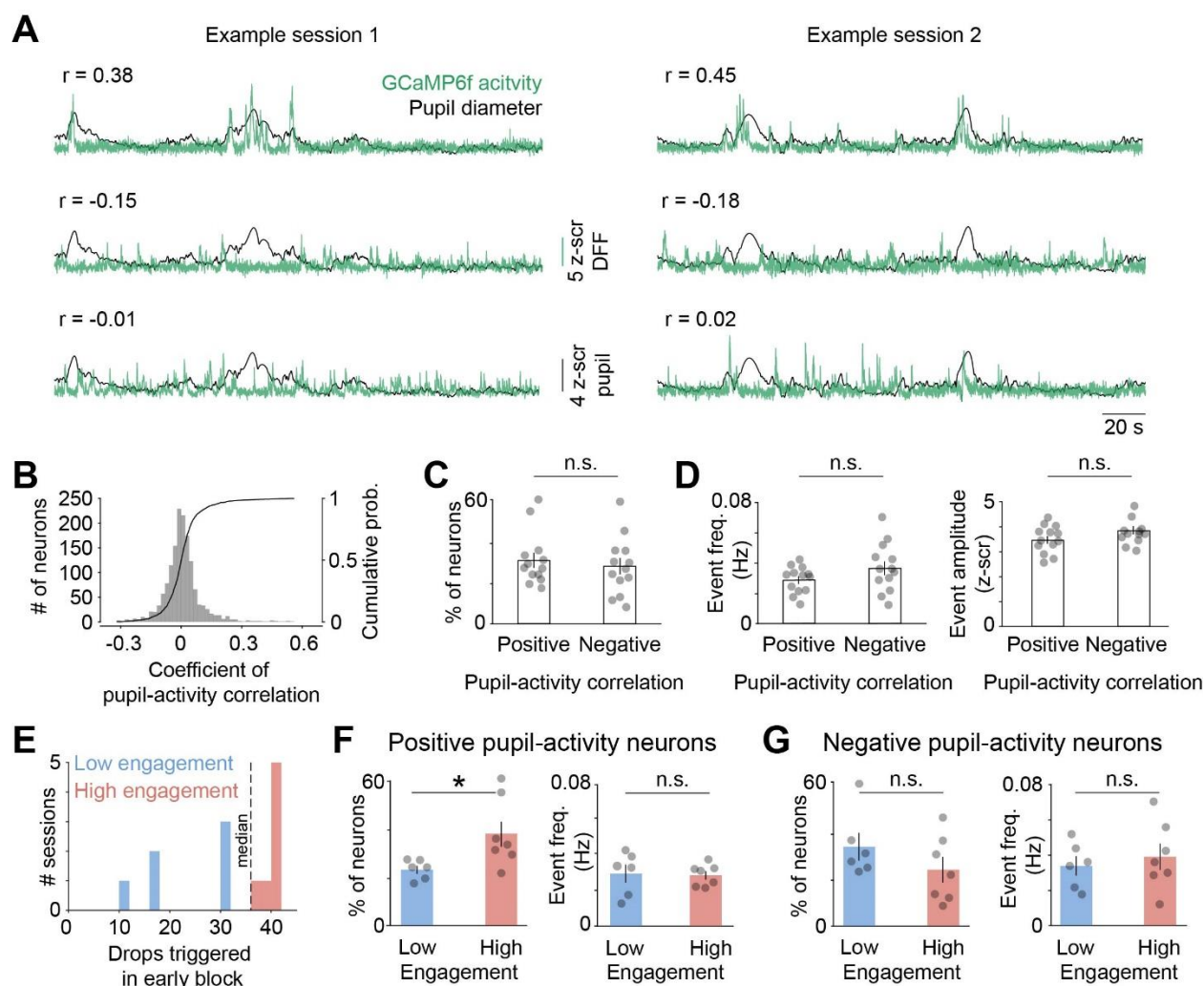
404

17

405 **Figure 1. Head-fixed mice voluntarily consume ethanol during two-photon imaging.** (A) Top:
406 timeline of the ‘drinking in the dark’ paradigm (DID) in relation to zeitgeber time (ZT). Regular
407 bottles were replaced with 20% ethanol (v/v) in drinking water for 3 hours beginning 3 hours into
408 the dark phase (ZT15, blue) with habituation occurring prior (ZT12, gray). Bottom: timeline of
409 head-fixed drinking (HFD). Animals were provided access at ZT15 for 3x10 minute sessions
410 consisting of pre, early (blue), and late (orange) ethanol access. (B) Ethanol consumption across
411 DID, DID with head-fixed habituation, and HFD periods. $n = 4$ mice. (C) Task structure for
412 voluntary ethanol delivery (ITI, intertrial interval). (D) Volume of ethanol consumed during early
413 and late drinking blocks (paired t-test, $t(11) = 0.77$, $p = 0.46$; $n = 12$ sessions from 4 mice). (E)
414 Schematic of imaging setup (bottom) with examples of drinking camera, 2-photon imaging, and
415 pupil camera.. (F) Example simultaneously measured DFF traces of an example neuron (green),
416 pupil size (black), ethanol delivery (blue), and the observed lick bouts (magenta). n.s., not
417 significant.



419 **Figure 2. Effect of ethanol consumption on single neuron ACC activity and pairwise**
420 **correlations.** (A) Activity of three example neurons during pre, early, and late drinking. Detected
421 calcium events (black) are shown overlaid on the z-scored DFF signal (green). (B) DFF event rates
422 during pre (gray) and late (orange) drinking for all neurons. Cumulative probability (prob.)
423 distribution ($p = 9 \times 10^{-18}$, $k = 0.1638$; $n = 1471$ neurons from 4 mice) and session-wide mean of
424 events rates ($p = 0.88$, $z = -0.16$; $n = 12$ sessions from 4 mice) is shown. (C) Same as B, except for
425 neurons with increased activity modulated by ethanol (prob. distribution, $p = 10^{-47}$, $k = 0.82$, $n =$
426 158 neurons from 4 mice; mean event rates, $p = 0.002$; $z = -3.06$; $n = 12$ sessions from 4 mice).
427 (D) Same as B, except for neurons with decreased activity modulated by ethanol (prob. distribution,
428 $p = 10^{-43}$, $k = 0.69$, $n = 202$ neurons from 4 mice; mean event rates, $p = 0.002$; $z = 3.06$; $n = 12$
429 sessions from 4 mice). (E) Raster plot showing detected events for neurons with significantly
430 increased activity across drinking (top). Rows show activity for individual neurons. Mean event
431 rates in 1 min bins averaged across all increased activity neurons are shown below. (F) Same as E,
432 except for decreased activity neurons. (G) Color plot showing the trial-averaged activity of neurons
433 (rows) showing increased activity around the time of ethanol delivery. (H) Same as G, except for
434 neurons showing decreased activity around ethanol delivery. (I) z-scored DFF averaged across
435 neurons with increased (green) and decreased (magenta) activity that are shown in G and H,
436 respectively. (J) Example field of view (FOV), noting the spatial location of four representative
437 neurons (white circles/numbers). (K) The activity of pairs of neurons shown in J for pre-drinking
438 and late drinking blocks. (L) Mean pairwise correlation coefficients averaged for all unique pairs
439 during individual pre- and late drinking blocks ($p = 0.18$, $z = -1.33$, $n = 12$ sessions from 4 mice;
440 Wilcoxon signed-rank test). In B-D, comparison of cumulative probability distributions with two-
441 tailed, two-sample Kolmogorov-Smirnov test and comparison of means with two-tailed Wilcoxon
442 signed-rank test. *** $p < 0.005$, n.s., not significant.



443

444 **Figure 3. Pupil-activity correlation during pre-drinking is associated with subsequent**

445 **engagement with ethanol.** (A) Traces of pupil diameter (z-scored, black) overlaid on GCaMP6f

446 DFF responses (z-scored, green) of representative neurons from two example sessions showing

447 varying levels of pupil-activity coupling. (B) Histogram (left y-axis) and cumulative probability

448 distribution (right y-axis) for Pearson correlation coefficient between fluctuations in neuronal

449 activity and pupil diameter ($n = 1519$ neurons from 4 mice). (C) Percentage of neurons with

450 significant positive and negative activity-pupil correlations ($n = 13$ sessions from 4 mice; $p = 0.78$,

451 $z = 0.28$). (D) DFF event frequency (left; $p = 0.20$, $z = -1.28$) and amplitude (right; $p = 0.20$, $z = -$

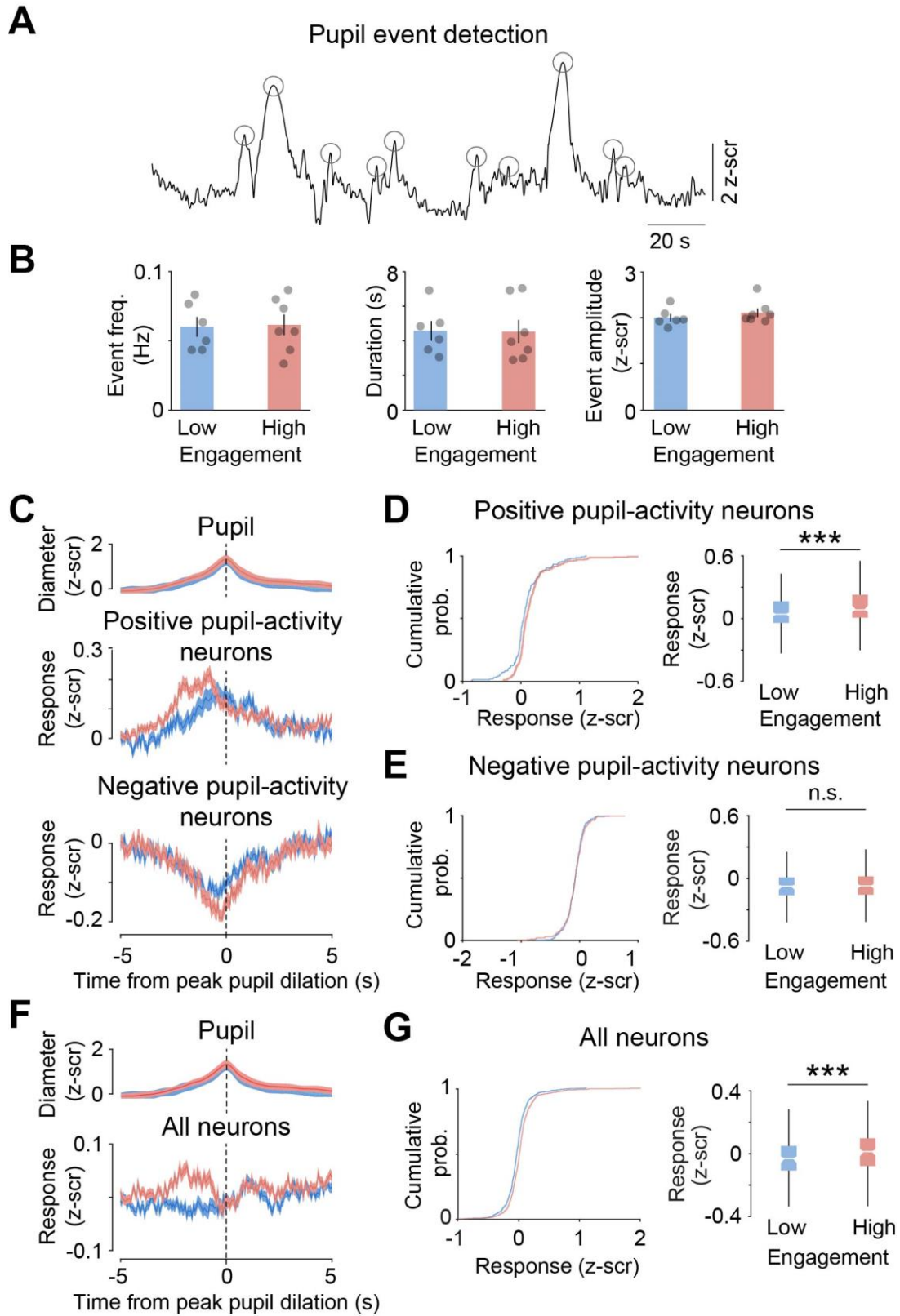
452 1.28) for positively and negatively coupled neurons ($n = 13$ sessions from 4 mice). (E) High (red)

453 and low (blue) ethanol engagement sessions were defined based on median split of the number of

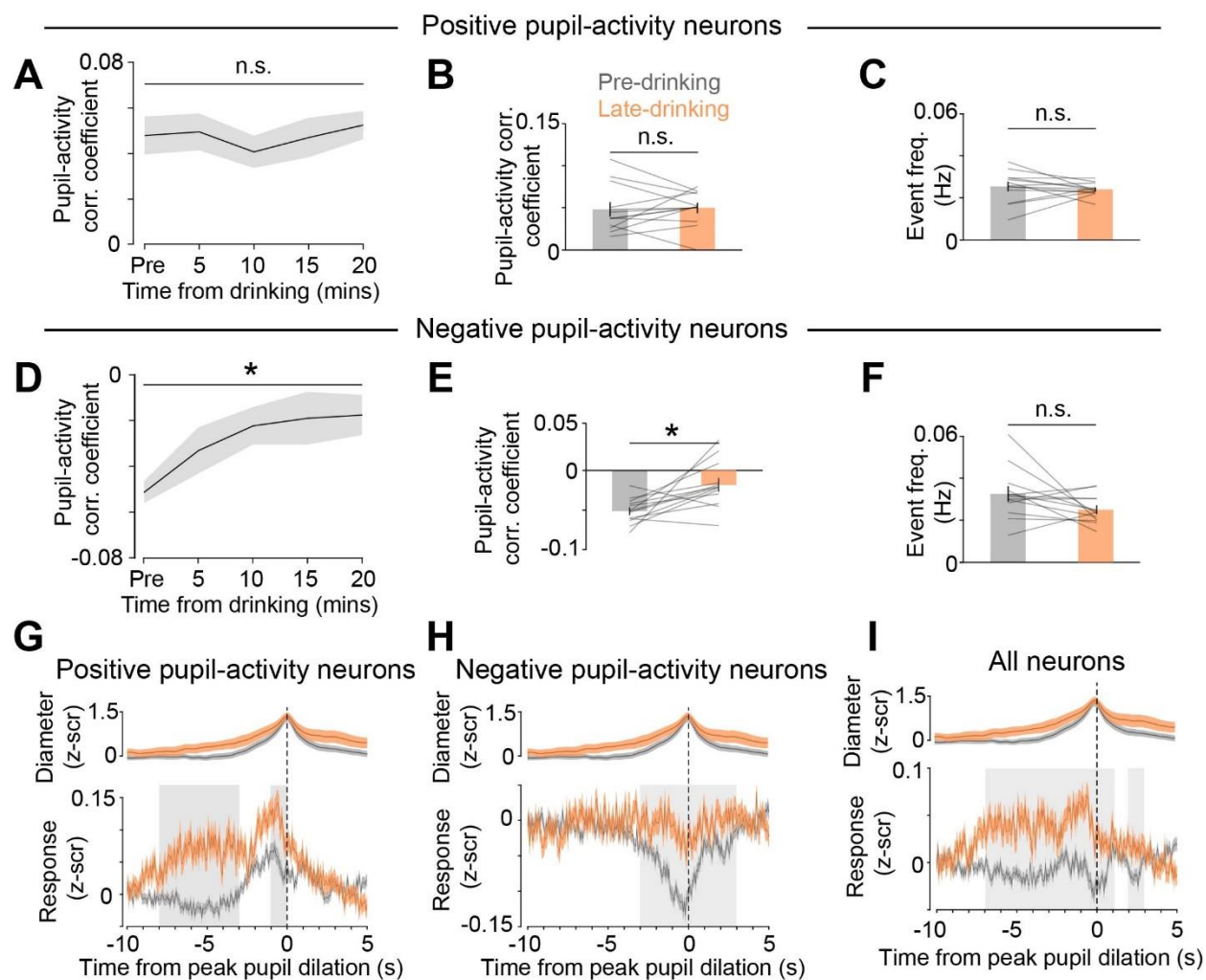
454 ethanol drops triggered during early drinking (high, 7 sessions from 4 mice; low, 6 sessions from

455 3 mice). (F) Percentage of neurons with positive coupling to pupil in low and high engagement

456 sessions ($p = 0.02$, $z = -2.36$) and their DFF event rates in the two sessions ($p = 0.52$, $z = 0.64$) (G)
457 Same as F, but for neurons with negative pupil-activity correlations (percent of neurons, $p = 0.23$,
458 $z = 1.21$; event rate, $p = 0.83$, $z = -0.21$). Statistical testing with two-tailed Wilcoxon rank-sum
459 tests in all panels. * $p < 0.05$, n.s., not significant.

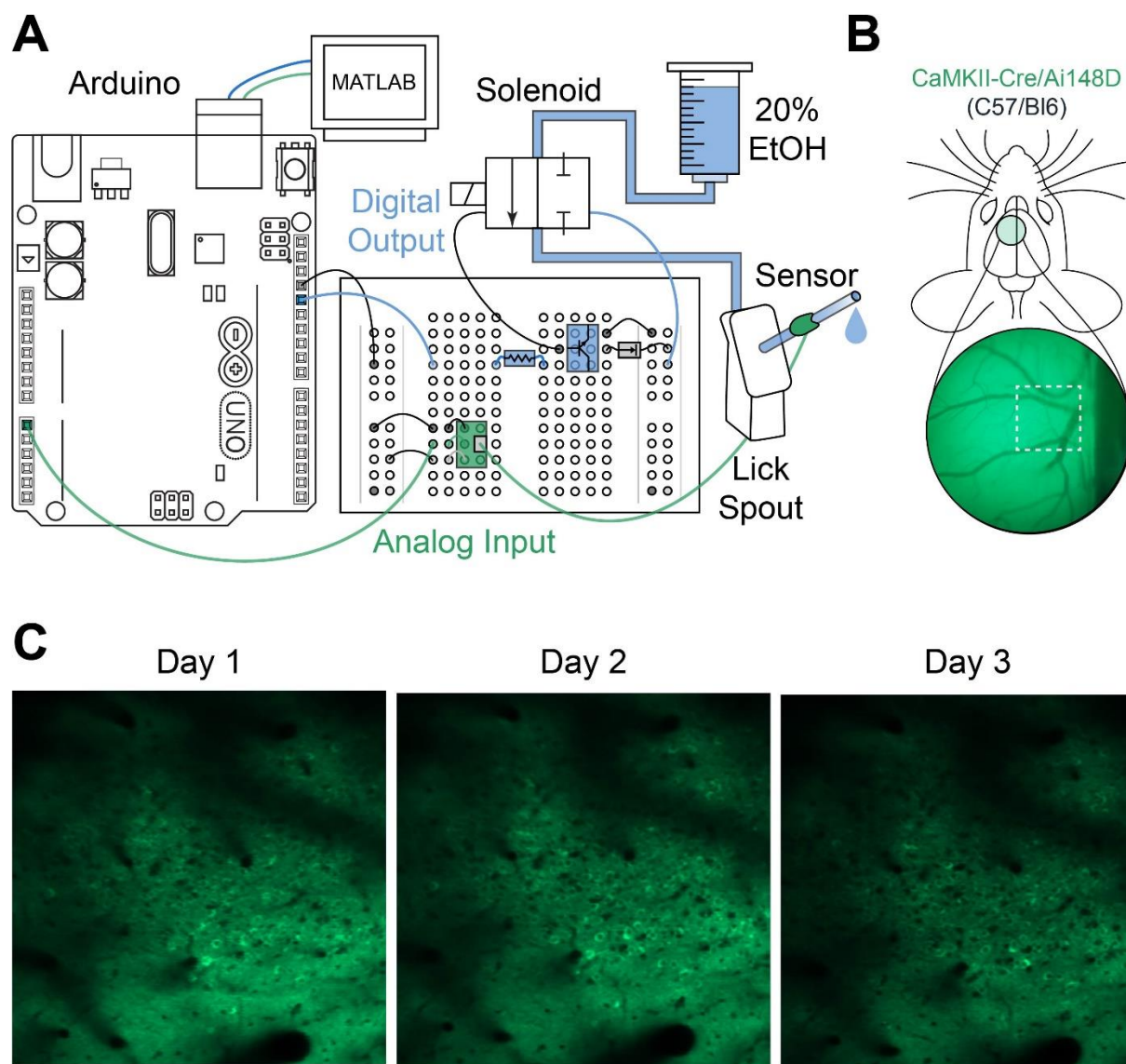


461 **Figure 4. Pupil-aligned neuronal responses during pre-drinking are associated with**
462 **subsequent ethanol engagement.** (A) Trace of pupil diameter (z-scored, black) from an example
463 session showing peaks of individual dilation events (circles). (B) Quantification of pupil event rate
464 ($p = 0.94$, $z = -0.07$), duration ($p = 0.62$, $z = 0.5$), and amplitude ($p = 0.35$, $z = -0.92$) for low (blue)
465 and high (red) engagement sessions ($n = 7$ high sessions from 4 mice, 6 low sessions from 3 mice).
466 (C) Session-averaged pupil events (top) and neuronal responses from positively (middle; low, $n =$
467 171 neurons from 3 mice; high, $n = 297$ neurons from 4 mice) and negatively (bottom; low, $n =$
468 242 neurons from 3 mice; high, $n = 212$ neurons from 4 mice) coupled neurons, with signals
469 aligned to the peak of pupil dilation events. Responses from low (blue) and high (red) engagement
470 sessions are shown. (D) Cumulative probability distribution (left panel; $p = 0.00013$, $k = 0.21$) and
471 median (right panel; $p = 0.002$, $z = -3.17$) pupil-aligned responses averaged over a window of -2
472 to -1s relative to peak pupil dilation. (E) Same as D, except for negatively coupled neurons
473 (cumulative distribution: $p = 0.92$, $k = 0.05$; box plot: $p = 0.85$, $z = -0.19$). (F) Same as C, except
474 for all neurons regardless of correlation with the pupil (low, $n = 718$ neurons from 3 mice; high, n
475 = 801 neurons from 4 mice). (G) Same as D, except for all neurons (cumulative distribution, $p =$
476 2×10^{-9} , $k = 0.16$; box plot, $p = 5 \times 10^{-9}$, $z = -5.84$). Box plot elements: center line, median; box
477 limits, upper and lower quartiles; whiskers, 1.5x interquartile range; outliers not shown).
478 Comparisons in B and the box plots in D, E, G with two-tailed Wilcoxon rank-sum test;
479 significance testing of cumulative distributions in D, E, G with two-tailed, two-sample
480 Kolmogorov-Smirnov test. *** $p < 0.005$, n.s., not significant.



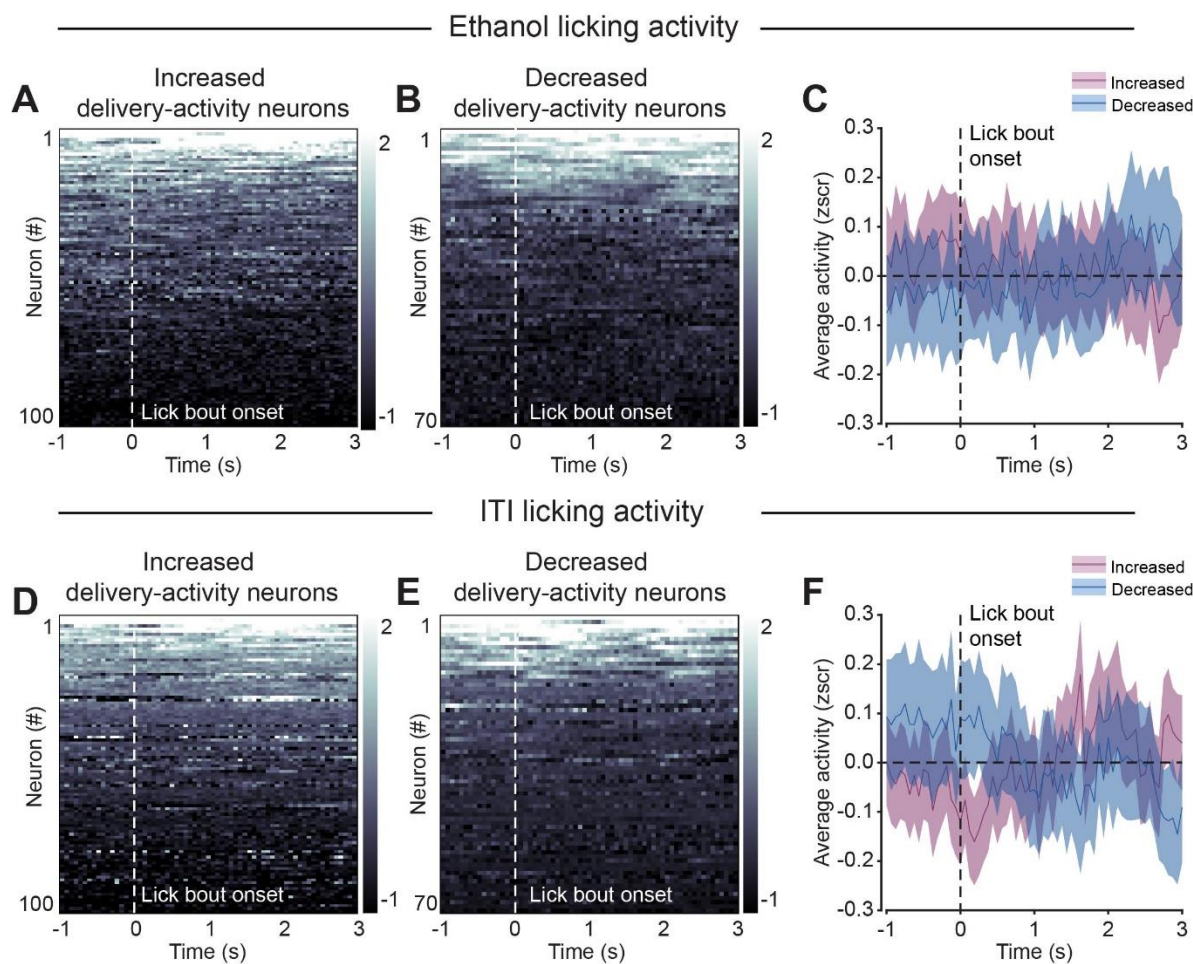
481
482 **Figure 5. Voluntary ethanol consumption disrupts neuronal-arousal coupling.** (A) Session-
483 averaged correlation (corr.) coefficients for positive pupil-activity modulated neurons, quantified
484 in 5 min bins across drinking ($H(4,55) = 2.13$, $p = 0.71$; $n = 12$ sessions from 4 mice). (B) Average
485 pupil-activity correlation coefficients during pre-drinking and last 5 minutes of late-drinking ($p =$
486 0.81 , $z = -0.24$). (C) DFF event frequency for pre-drinking (gray) and late (orange) drinking block
487 ($p = 0.48$, $z = 0.71$). (D, E, F) Same as A, B, C except for negative pupil-activity neurons (panel
488 D, $H(4,55) = 9.7$, $p = 0.046$; panel E, $p = 0.012$, $z = -2.51$; panel F, $p = 0.14$, $z = 1.49$). (G) Pupil
489 responses (z-scored, top) and pupil-aligned activity (z-scored, bottom) of neurons with significant
490 positive pupil-activity correlations during pre- and late drinking. Activity was compared in 1s
491 windows using two-tailed Wilcoxon signed-rank test; gray shading denotes windows with
492 significant difference between the two blocks using Bonferroni corrected α -value of 0.0033
493 (0.05/15). (H, I) Same as G, except for negative pupil-activity neurons (H) and all recorded neurons

494 (I). Significant testing with Kruskal-Wallis test in A and D, and with Wilcoxon signed-rank test in
495 B, C, E, and F. * $p < 0.05$, n.s., not significant.



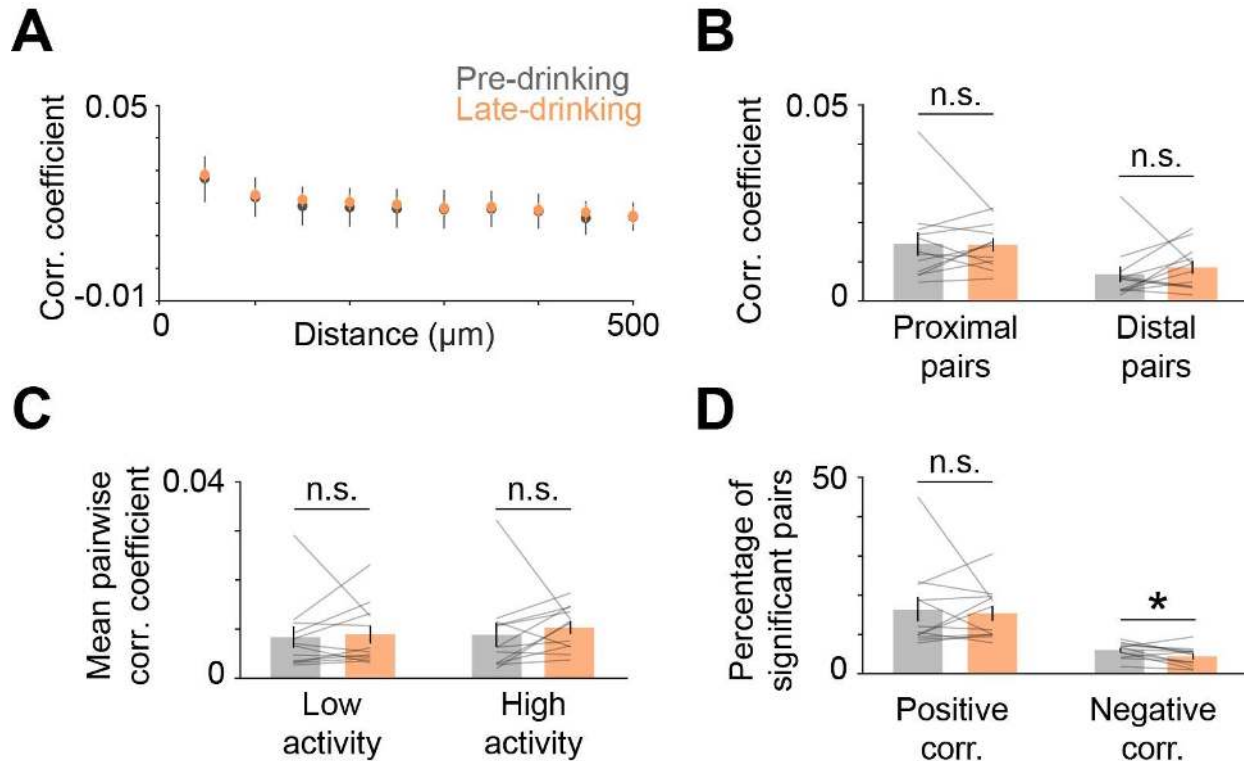
496

497 **Supplementary Figure 1. Voluntary ethanol engagement with cortical imaging over days.** (A)
498 Circuit diagram for lick detection (analog input, green) and ethanol delivery (digital output, blue).
499 (B) Example low-magnification field of view of anterior cingulate cortex (ACC) and imaging
500 region (white dashed box). (C) Example imaging of excitatory ACC neurons across 3 days.
501 Coordinates of 0.5mm anterior to Bregma and 0.3mm lateral to the midline were targeted using
502 recorded imaging depth, vasculature shadow patterns, and background fluorescence of neuronal
503 somata.



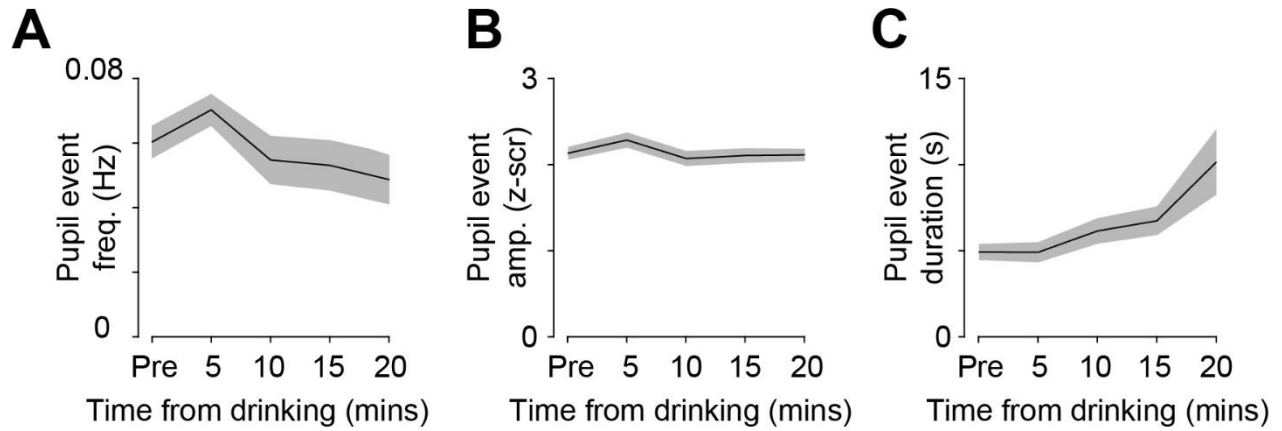
504

505 **Supplementary Figure 2. Licking does not significantly modulate neuronal activity.** (A)
506 Activity of neurons with increased ethanol delivery-activity shown in Fig. 2G but aligned to licking
507 bouts occurring around ethanol delivery. (B) Same as A, but for neurons with decreased delivery-
508 activity neurons shown in Fig. 2H. (C) Averaged DFF responses of increased (green) and
509 decreased (magenta) delivery-activity neurons (as in Fig. 2I), but aligned to lick bouts around
510 ethanol delivery. (D, E, F) Same as A, B, C but aligned to licking bouts in the inter-trial interval
511 (ITI).



512

513 **Supplementary Figure 3. Effect of ethanol consumption on pairwise activity correlations.** (A)
514 Session-averaged pairwise correlation coefficients between all unique pairs of simultaneously
515 recorded neurons binned by the distance between neurons in each pair (bin size, 50 μm). (B)
516 Activity correlations of proximal (<50 μm apart) and distal (>300 μm apart) pairs during pre (gray)
517 and late (orange) drinking (proximal, $p = 0.58$, $z = -0.55$; distal, $p = 0.21$, $z = -1.26$). (C)
518 Comparison of correlation coefficients of pairs with low and high activity, defined based on the
519 median split of the calcium event frequency averaged across the neurons in a pair (low activity, p
520 $= 0.88$, $z = -0.15$; high activity, $p = 0.07$, $z = -1.80$). (D) Percentage of neuronal pairs with
521 significant positive or negative pairwise correlations (positive, $p = 0.94$, $z = -0.08$; negative, $p =$
522 $.0041$, $z = 2.04$). Error bars are standard error of the mean ($n = 12$ sessions from 4 mice).
523 Significant testing with Wilcoxon rank-sum test; * $p < 0.05$; n.s., not significant.



524

525 **Supplementary Figure 4. The effect of drinking on pupil dynamics.** (A-C) Frequency ($H(4,55)$
526 $= 6.82$, $p = 0.14$), amplitude ($H(4,55) = 4.71$, $p = 0.22$), and duration ($H(4,55) = 8.95$, $p = 0.06$) of
527 detected pupil dilation events in 5 min bins across drinking ($n = 12$ sessions from 4 mice).
528 Significance testing with one-way Kruskal-Wallis test.

529

530 **Supplementary Video 1. Home-cage video of mice after voluntary head-fixed ethanol**
531 **consumption.**

532 **Methods**

533 **Mice:** Animals expressing GCaMP6f under the CaMKII promoter were generated by crossing the
534 commercially available Camk2a-Cre (005359, Jackson) and Ai148D (030328, Jackson) mouse
535 lines, both on a C57/B16 background. Animals were maintained in their home cages under a 12/12
536 reverse light/dark cycle with *ad libitum* access to standard mouse chow and water. All animals
537 used in this study were ~P60 male mice. All animal procedures were performed in strict accordance
538 with protocols approved by the MIT Division of Comparative Medicine and conformed to NIH
539 standards.

540 **Surgical Procedures:** Surgeries were performed under isoflurane anesthesia (3% induction, 1.5%
541 maintenance) and body temperature was maintained at 37.5°C using a temperature controller
542 (ATC2000, World Precision Instruments). Animals were dosed with slow-release buprenorphine
543 (0.1mg/kg) prior to surgery, and meloxicam (1mg/kg) every 24 hours post-surgery for 72 hours or
544 until fully recovered. Once stably anesthetized, animals were head-fixed in a stereotaxic frame
545 (51500D, Stoelting), scalp hair removed, and scalp sterilized using alternating betadine scrub and
546 70% ethanol solutions. A portion of the scalp was removed and conjunctive tissue cleared after
547 treatment with hydrogen peroxide. A 3mm diameter craniotomy was then drilled over centered
548 over left ACC/M2 (from bregma, AP: 1.0mm, ML: 1.0mm). A chronic cranial window was then
549 implanted that consisted of a 5mm diameter coverslip glued to two 3mm coverslips (Warner
550 Instruments) using optical UV-cured adhesive (61, Norland). The window was carefully lowered
551 with the 5mm coverslip on top and firmly held in the craniotomy using the stereotax while adhered
552 to the skull using dental acrylic mixed with black ink (Metabond, Parkell). Once the dental acrylic
553 had cured around the cranial window, a custom stainless-steel head-fixation plate was mounted
554 around the cranial window and cured with dental acrylic. Animals were then allowed to recover in
555 their own cage with a warm water blanket and moistened food chow. Mice were singly housed for
556 the remainder of the experiment and continued to recover for one week before beginning the
557 drinking in the dark paradigm.

558 **Drinking in the dark (DID) paradigm:** Following recovery from window implantation, mice
559 were introduced to the drinking in the dark paradigm (DID) as previously described for 13 days.
560 Mice were weighed, and their water bottles replaced with 15ml conical tubes containing 20%
561 ethanol (v/v) diluted in the mouse drinking water 3 hours into their dark phase (ZT15). Tubes were

562 filled with ~10mL of ethanol solution, fitted with a custom rubber stopper and standard lick spout,
563 and then weighed before being placed in each cage. One drop of ethanol solution was allowed to
564 drip to ensure the displacement of air. A control cage without any mice was also fitted with an
565 ethanol drinking tube to account for the displacement drop and evaporation. Mice were then left
566 alone for 3 hours during which they could voluntarily consume the ethanol solution. After 3 hours,
567 the ethanol tubes were removed, weighed, and regular drinking water bottles returned. The amount
568 of ethanol consumed was calculated by subtracting the final weight from the initial weight of each
569 tube to get a session difference. The control tube difference was then subtracted from each mouse
570 tube difference, and then consumption computed as ethanol consumed (g) per weight of the animal
571 (kg). After 9 days of normal DID exposure, mice were head-fixed on the two-photon imaging rig
572 for 30 minutes (ZT 12-15) prior to the DID paradigm (ZT15) for 5 days to habituate the mice to
573 the imaging setup.

574 **Head-fixed drinking paradigm:** After animals completed 13 days of DID, last 5 days of which
575 they were habituated to head-fixation, mice were imaged while voluntarily consuming ethanol
576 under the two-photon microscope. Animals were head-fixed on an elevated platform with a
577 lickspout delivering 20% EtOH (v/v) in mouse drinking water positioned within easy access for
578 licking. The lickspout was made from a brass tube (3.97mm diameter, 8128, K&S Precision
579 Metals) that was wrapped with conductive wire and connected to a capacitive sensor (P1374,
580 Adafruit) integrated to a breadboard and connected to an Arduino board (Uno Rev3, A000066,
581 Arduino) as an analog input and recorded via custom MATLAB scripts. Ethanol delivery was
582 initiated by custom MATLAB scripts that sent a digital signal via the Arduino to toggle a transistor
583 on the breadboard (IRF520PBF, Digi-Key) and open a 12V solenoid (VAC-100 PSIG, Parker).
584 Ethanol solution was maintained in a graduated syringe, gravity fed into the solenoid, and
585 calibrated to deliver a small drop (~8 μ L) with each trigger. Following each session, total ethanol
586 delivered was compared between the graduated syringe and the calculated trigger volume to ensure
587 accurate quantification of total ethanol delivered (for detailed circuit diagram and session structure
588 see Fig. 1 and Supp. Fig. 1).

589 For the initial sessions after switching from DID to head-fixed drinking, mice could lick
590 the spout to receive ethanol soon after head-fixation. To determine how drinking affects ACC
591 activity relative to before drinking, in later sessions we introduced a 10 minute pre-drinking
592 imaging block in which animals were allowed to lick the spout but no ethanol was delivered.

593 Following the pre-drinking block, animals underwent two subsequent 10 minute drinking blocks
594 in which licking the spout could deliver a drop of ethanol. The drinking blocks were structured
595 such that after initiation, there was a pseudorandom delay before a lick query (exponential
596 distribution with a 10s mean and cut-offs at 5s and 20s). If the animal had licked within 1s prior
597 to the query, a drop of ethanol solution was dispensed, otherwise an additional delay of 1s was
598 imposed before another lick query. Hence, the animal had to lick during the query period to trigger
599 ethanol delivery. This design promoted continuous licking of the spout in order to obtain more
600 ethanol, thereby limiting unconsumed ethanol delivery. Moreover, the self-paced design allowed
601 us to assess the animal's level of engagement with ethanol by quantifying the number of drops that
602 were triggered. A camera (LifeCam, Q2F-00013, Microsoft) was positioned to record licking
603 behavior and to validate that ethanol delivery was consumed. To quantify changes in arousal, an
604 infrared CMOS camera (DCC1545M, ThorLabs) was fitted with a telecentric lens (SilverTL, 58-
605 430, Edmund Optics) and positioned over the pupil for high-speed acquisition (20Hz) via custom
606 MATLAB scripts. The pupil was illuminated by an infrared LED array (LIU780A, ThorLabs).
607 Ethanol delivery, image acquisition, and pupil imaging were all synchronously triggered at the
608 start of the session to accurately align temporal epochs across measurements.

609 We analyzed data from sessions with imaging during both pre-drinking and drinking
610 blocks. We had 13 such sessions, which were included in the analysis of pre-drinking activity
611 (Figs. 3, 4). 1 session had poor quality imaging data in the late drinking block and hence was
612 excluded from data presented in Figs. 2 and 5.

613 **Measurement of blood ethanol concentration:** Blood ethanol concentration (BEC) was
614 quantified after the final imaging session. Immediately the session, animals were rapidly
615 anesthetized by isoflurane, decapitated, and whole trunk blood collected in tubes lined with EDTA
616 (BD Microtainer, 365974, Becton, Dickinson and Company) and placed on ice. Whole blood was
617 then centrifuged at 3000xg for 10 minutes at 4°C. Separated plasma was then aliquoted and
618 immediately stored at -80°C for further analysis. Quantification of BEC was performed using a
619 colorimetric assay as previously described. Ethanol standards and plasma samples were diluted in
620 sample reagent (all reagents obtained from Millipore Sigma): 100mM KH₂PO₄ (P3786), 100mM
621 K₂HPO₄ (P3786), 0.7mM 4-aminoantropyrine (A4382), 1.7mM chromotropic acid (27150),
622 50mg/L EDTA (E4884), and 50mL/L Triton X100 (X100). Working reagent was created by
623 mixing alcohol oxidase from *Pichia* (5kU/L, A2404) and horseradish peroxidase (3kU/L, 77332)

624 with sample reagent and mixed with samples on a 96-well plate. Following 30 minutes of
625 incubation at room temperature, the samples and standards were read on a standard plate reader
626 (iMark, Bio-Rad Laboratories) at 595nm. Samples and standards were run 6x in parallel and BEC
627 calculated according to the standard curve.

628 **Two-Photon calcium imaging:** GCaMP6f fluorescence from neuronal somas was imaged through
629 a 16x/0.8 NA objective (Nikon) using resonance-galvo scanning with a Prairie Ultima IV two-
630 photon microscopy system. Image frames were collected as 4-frame averages at 480x240 pixel
631 resolution an acquisition rate of 16Hz. Excitation light at 900nm was provided by a tunable
632 Ti:Sapphire laser (Mai-Tai eHP, Spectra-Physics) with ~10-20 mW of power at sample. Emitted
633 light was filtered using a dichroic mirror (collected with GaAsP photomultiplier tubes
634 (Hamamatsu). Layer 2/3 GCaMP6f-expressing neurons were imaged with 1.5x optical zoom, 120-
635 200 μ m below the brain surface. Neuronal activity in the ACC was collected at the following
636 coordinates: ~0.5mm AP, ~0.5mm ML.

637 **GaMP6f fluorescence signal processing:** We used the software Suite2P¹¹¹ for semi-automatic
638 detection of neuronal somas from calcium imaging movies. Movies from the three imaging blocks
639 were concatenated together and the non-rigid translation function in Suite2P was used to correct
640 for x-y translations that may have occurred between blocks. Suite2P detects neuronal regions of
641 interest (ROI) by clustering neighboring pixels with similar fluorescence time courses. Moreover,
642 it provides for each detected neuron a neuropil mask which surrounds the detected ROI and
643 excludes other detected neuronal ROIs. The automatically detected ROIs were manually curated
644 using the GUI such that ROIs without clear visual evidence for neuronal somas were rejected and
645 neurons missed by the algorithm were added manually.

646 To minimize the contribution of the neuropil signal to the somatic signal, corrected
647 neuronal fluorescence at each time point t was estimated as $F_t = F_{raw_soma_t} - (0.3 \times$
648 $F_{raw_neuropil_t})^{112}$. The DFF ($\Delta F/F$) for each neuron was calculated as $\Delta F/F(t) = 100 \times (F(t) -$
649 $F_0)/F_0$, where F_0 represents the mode of the distribution of fluorescence values (estimated using
650 the MATLAB function 'ksdensity'). The resulting DFF trace was z-scored. We identified
651 individual calcium events as transient increases in the z-scored DFF signal. Using the 'findpeaks'
652 function in MATLAB, we detected events with minimum peak prominence of 2.5 z-scored DFF

653 and minimum width of 3 imaging frames (~200ms) at half-height of the event peak. All analyses
654 either used the z-scored DFF or detected calcium event frequency and amplitude.

655 **Analysis of change in neuronal activity with ethanol consumption:** We tested how ethanol
656 consumption affects neuronal activity over the slow time scale of minutes across the entire imaging
657 session. A challenge with this analysis is that the pre-drinking block has no trial structure, making
658 it difficult to align activity to specific events and statistically compare how drinking affects
659 activity. While one strategy is to compare inter-event intervals between pre-drinking and drinking
660 blocks, we reasoned that the sparse cortical activity observed in individual blocks would be a
661 limiting factor and produce false negatives. Hence, we instead addressed this issue by devising a
662 shuffle test. This test circularly shifted traces of detected calcium events in time by a random
663 amount in intervals of 30s, thus maintaining the temporal structure of activity while randomizing
664 the timing at which it occurred. We reiterated this process 1000 times for each neuron. On every
665 iteration, we computed the difference in event frequency between pre-drinking and 1) the first
666 drinking block; and 2) the second drinking block. This allowed us to generate null distributions for
667 the difference in event frequency expected by chance given the overall activity level of the neuron.
668 The two-tailed p-value for each drinking block was computed as the proportion of activity changes
669 in the null distribution that were as or more extreme than the experimentally observed change on
670 either side of the distribution. Neurons with $p < 0.05$ for either drinking block were considered
671 significant and classified as positively or negatively modulated depending on how their activity
672 changed with drinking.

673 We also tested how individual ACC neurons were modulated on a faster time scale, around
674 the time of ethanol consumption and licking. We aligned neuronal activity to the time of ethanol
675 delivery and compared responses 1s before and after delivery using a one-tailed Wilcoxon signed-
676 rank test to identify positively or negatively modulated neurons. Neurons with $p < 0.01$ were
677 considered significant. We similarly aligned responses to licking bouts occurring at any time,
678 during a 4s window after ethanol delivery, or during the inter-trial delay (i.e., 4s after ethanol
679 delivery). Licking bouts were defined as two or more consecutive licks that occurred with a delay
680 of less than 500ms.

681 **Pairwise neuronal correlation analysis:** We assessed the effect of ethanol consumption on
682 Pearson correlations between the z-scored DFF traces for all unique pairs of neurons in each

683 recording session. To facilitate comparison between drinking and pre-drinking blocks, activity 3s
684 after ethanol delivery in the drinking blocks was not included in the analysis. Correlations were
685 computed using the last 5 minutes of the pre and late drinking blocks. Pair-wise correlations of all
686 simultaneously recorded pairs in a single session were averaged together separately for the pre-
687 drinking and drinking blocks. These session-averaged values were then compared between the
688 blocks using a Wilcoxon signed-rank test. We quantified pair-wise correlations as a function of
689 the distance between neurons in each pair. We calculated the Euclidean distance between each pair
690 of neurons as the length of a straight line connecting the center coordinates of each neuronal ROI.
691 We defined proximal pairs as neurons less than 50 μm apart and distal pairs as neurons with more
692 than 300 μm distance between them. We also analyzed whether the overall level of activity in the
693 pair of neurons is related to ethanol's effect on pair-wise correlations. We did a median-split for
694 the average event frequency for each pair and compared pair-wise correlations separately for pairs
695 with high and low levels of activity. Lastly, we quantified and compared the proportion of neuron
696 pairs with significant positive or negative pair-wise correlations during pre-drinking and post-
697 drinking ($p < 0.05$).

698 **Neuronal-arousal coupling analysis:** We performed two types of analyses to study the
699 relationship between neuronal-arousal coupling and ethanol consumption: 1) correlation between
700 fluctuations in pupil size and neuronal activity; 2) analysis of pupil-aligned neuronal activity. The
701 pupil was imaged at a frequency 20Hz. We downsampled the pupil signal to match the frequency
702 of two-photon calcium imaging data (~ 16 Hz) using the MATLAB function 'interp1'. For activity-
703 pupil correlation analysis, we determined the Pearson correlation coefficient between neuronal
704 activity and traces of z-scored pupil diameter. To evaluate the association of neuronal-arousal
705 coupling during the pre-drinking block with subsequent drinking, we separately analyzed sessions
706 with high and low levels of drinking, which were defined based on the median split of the total
707 number of ethanol drops triggered by the animal in the first drinking block. Neurons were defined
708 as positively or negatively modulated if they had a significant correlation with the pupil ($p < 0.05$)
709 and depending on the sign of their correlation coefficient. Pre-drinking activity-pupil correlations
710 were quantified for the second half of the pre-drinking block (i.e., last 5 minutes).

711 For tracking how correlations evolve across pre-drinking and drinking, we computed
712 activity-pupil correlations coefficients in 5 min bins starting from the last 5 minutes of the pre-
713 drinking to the end of the late drinking block. To facilitate comparison between pre-drinking and

714 drinking blocks, neuronal and pupil data from 3s after each ethanol drop delivery during the
715 drinking block were excluded from the analysis. Neurons with significant positive or negative
716 correlations in any of the bins were included in the analysis ($p < 0.05$).

717 To analyze pupil-aligned neuronal activity, we first identified individual dilation events in
718 traces of z-scored pupil diameter using the MATLAB function ‘interp1’ with a threshold
719 prominence of 1 z-score. This allowed us to quantify the pupil dilation event rate, duration, and
720 amplitude, in addition to identifying the time at which the peak of the dilation event occur.
721 Neuronal responses were aligned to this peak time. For pre-drinking analysis, pupil-aligned
722 responses for each neuron were averaged for all pupil events occurring in the last 5 mins of the
723 block; for late drinking, last 5 mins of the second drinking block was used.

724 **Data availability**

725 The data that support the findings of this study are available from the corresponding author upon
726 reasonable request.

727 **Code availability**

728 Custom code used in this work is available from the corresponding author upon reasonable request.

729 **Acknowledgements**

730 This work was supported by grants from National Eye Institute F32EY028028 to G.O.S.; from
731 National Institute of Mental Health R00MH104716 to E.V. and MH112855 to R.H.; and National
732 Institute on Alcohol Abuse and Alcoholism U01AA025481 to E.V. We thank Mriganka Sur for generously
733 providing the use of his laboratory for these experiments.

734 **Author contributions**

735 G.O.S. and R.H. conceived the project, designed the experiments, and developed the concepts
736 presented. G.O.S. performed the experiments with contributions from R.H. and E.V. R.H.
737 performed the analysis with contributions from G.O.S., I.L. and M.N. E.V. provided feedback on
738 overall experimental design and data interpretation. R.H. and G.O.S. wrote the manuscript with
739 input from all authors.

740 **Competing interests**

741 The authors declare no competing interests.

742 References

- 743 1 Rhodes, J. S., Best, K., Belknap, J. K., Finn, D. A. & Crabbe, J. C. Evaluation of a simple
744 model of ethanol drinking to intoxication in C57BL/6J mice. *Physiol Behav* **84**, 53-63,
745 doi:10.1016/j.physbeh.2004.10.007 (2005).
- 746 2 Thiele, T. E. & Navarro, M. "Drinking in the dark" (DID) procedures: a model of binge-
747 like ethanol drinking in non-dependent mice. *Alcohol* **48**, 235-241,
748 doi:10.1016/j.alcohol.2013.08.005 (2014).
- 749 3 Sprow, G. M. & Thiele, T. E. The neurobiology of binge-like ethanol drinking: evidence
750 from rodent models. *Physiol Behav* **106**, 325-331, doi:10.1016/j.physbeh.2011.12.026
751 (2012).
- 752 4 Simms, J. A. *et al.* Intermittent access to 20% ethanol induces high ethanol consumption
753 in Long-Evans and Wistar rats. *Alcohol Clin Exp Res* **32**, 1816-1823, doi:10.1111/j.1530-
754 0277.2008.00753.x (2008).
- 755 5 Huynh, N., Arabian, N. M., Asatryan, L. & Davies, D. L. Murine Drinking Models in the
756 Development of Pharmacotherapies for Alcoholism: Drinking in the Dark and Two-bottle
757 Choice. *J Vis Exp*, doi:10.3791/57027 (2019).
- 758 6 Crabbe, J. C., Harris, R. A. & Koob, G. F. Preclinical studies of alcohol binge drinking.
759 *Ann N Y Acad Sci* **1216**, 24-40, doi:10.1111/j.1749-6632.2010.05895.x (2011).
- 760 7 Alexander, W. H. & Brown, J. W. Medial prefrontal cortex as an action-outcome predictor.
761 *Nat Neurosci* **14**, 1338-1344, doi:10.1038/nn.2921 (2011).
- 762 8 Dixon, M. L., Thiruchselvam, R., Todd, R. & Christoff, K. Emotion and the prefrontal
763 cortex: An integrative review. *Psychol Bull* **143**, 1033-1081, doi:10.1037/bul0000096
764 (2017).
- 765 9 Miller, E. K. & Cohen, J. D. An integrative theory of prefrontal cortex function. *Annu Rev*
766 *Neurosci* **24**, 167-202, doi:10.1146/annurev.neuro.24.1.167 (2001).
- 767 10 Bechara, A. *et al.* Decision-making deficits, linked to a dysfunctional ventromedial
768 prefrontal cortex, revealed in alcohol and stimulant abusers. *Neuropsychologia* **39**, 376-
769 389, doi:10.1016/s0028-3932(00)00136-6 (2001).
- 770 11 George, O. & Koob, G. F. Individual differences in prefrontal cortex function and the
771 transition from drug use to drug dependence. *Neurosci Biobehav Rev* **35**, 232-247,
772 doi:10.1016/j.neubiorev.2010.05.002 (2010).
- 773 12 Ridderinkhof, K. R. *et al.* Alcohol consumption impairs detection of performance errors in
774 mediofrontal cortex. *Science* **298**, 2209-2211, doi:10.1126/science.1076929 (2002).
- 775 13 Park, S. Q. *et al.* Prefrontal cortex fails to learn from reward prediction errors in alcohol
776 dependence. *J Neurosci* **30**, 7749-7753, doi:10.1523/JNEUROSCI.5587-09.2010 (2010).
- 777 14 Wilcox, C. E., Dekonenko, C. J., Mayer, A. R., Bogenschutz, M. P. & Turner, J. A.
778 Cognitive control in alcohol use disorder: deficits and clinical relevance. *Rev Neurosci* **25**,
779 1-24, doi:10.1515/revneuro-2013-0054 (2014).
- 780 15 Jedema, H. P. *et al.* The acute impact of ethanol on cognitive performance in rhesus
781 macaques. *Cereb Cortex* **21**, 1783-1791, doi:10.1093/cercor/bhq244 (2011).
- 782 16 Pava, M. J. & Woodward, J. J. Chronic ethanol alters network activity and
783 endocannabinoid signaling in the prefrontal cortex. *Front Integr Neurosci* **8**, 58,
784 doi:10.3389/fnint.2014.00058 (2014).
- 785 17 Salling, M. C. *et al.* Alcohol Consumption during Adolescence in a Mouse Model of Binge
786 Drinking Alters the Intrinsic Excitability and Function of the Prefrontal Cortex through a

- 787 Reduction in the Hyperpolarization-Activated Cation Current. *J Neurosci* **38**, 6207-6222,
788 doi:10.1523/JNEUROSCI.0550-18.2018 (2018).
- 789 18 Robinson, S. L. *et al.* Medial prefrontal cortex neuropeptide Y modulates binge-like
790 ethanol consumption in C57BL/6J mice. *Neuropsychopharmacology* **44**, 1132-1140,
791 doi:10.1038/s41386-018-0310-7 (2019).
- 792 19 Lu, Y. L. & Richardson, H. N. Alcohol, stress hormones, and the prefrontal cortex: a
793 proposed pathway to the dark side of addiction. *Neuroscience* **277**, 139-151,
794 doi:10.1016/j.neuroscience.2014.06.053 (2014).
- 795 20 Cannady, R. *et al.* Interaction of chronic intermittent ethanol and repeated stress on
796 structural and functional plasticity in the mouse medial prefrontal cortex.
797 *Neuropharmacology* **182**, 108396, doi:10.1016/j.neuropharm.2020.108396 (2021).
- 798 21 Joshi, S. & Gold, J. I. Pupil Size as a Window on Neural Substrates of Cognition. *Trends*
799 *Cogn Sci* **24**, 466-480, doi:10.1016/j.tics.2020.03.005 (2020).
- 800 22 Reimer, J. *et al.* Pupil fluctuations track rapid changes in adrenergic and cholinergic
801 activity in cortex. *Nat Commun* **7**, 13289, doi:10.1038/ncomms13289 (2016).
- 802 23 Urai, A. E., Braun, A. & Donner, T. H. Pupil-linked arousal is driven by decision
803 uncertainty and alters serial choice bias. *Nat Commun* **8**, 14637,
804 doi:10.1038/ncomms14637 (2017).
- 805 24 Joshi, S., Li, Y., Kalwani, R. M. & Gold, J. I. Relationships between Pupil Diameter and
806 Neuronal Activity in the Locus Coeruleus, Colliculi, and Cingulate Cortex. *Neuron* **89**,
807 221-234, doi:10.1016/j.neuron.2015.11.028 (2016).
- 808 25 Reimer, J. *et al.* Pupil fluctuations track fast switching of cortical states during quiet
809 wakefulness. *Neuron* **84**, 355-362, doi:10.1016/j.neuron.2014.09.033 (2014).
- 810 26 McGinley, M. J., David, S. V. & McCormick, D. A. Cortical Membrane Potential Signature
811 of Optimal States for Sensory Signal Detection. *Neuron* **87**, 179-192,
812 doi:10.1016/j.neuron.2015.05.038 (2015).
- 813 27 Garcia-Junco-Clemente, P. *et al.* An inhibitory pull-push circuit in frontal cortex. *Nat*
814 *Neurosci* **20**, 389-392, doi:10.1038/nn.4483 (2017).
- 815 28 Larsen, R. S. & Waters, J. Neuromodulatory Correlates of Pupil Dilation. *Front Neural*
816 *Circuits* **12**, 21, doi:10.3389/fncir.2018.00021 (2018).
- 817 29 Batista-Brito, R., Zaghera, E., Ratliff, J. M. & Vinck, M. Modulation of cortical circuits by
818 top-down processing and arousal state in health and disease. *Curr Opin Neurobiol* **52**, 172-
819 181, doi:10.1016/j.conb.2018.06.008 (2018).
- 820 30 Cazettes, F., Reato, D., Morais, J. P., Renart, A. & Mainen, Z. F. Phasic Activation of
821 Dorsal Raphe Serotonergic Neurons Increases Pupil Size. *Curr Biol*,
822 doi:10.1016/j.cub.2020.09.090 (2020).
- 823 31 Dipoppa, M. *et al.* Vision and Locomotion Shape the Interactions between Neuron Types
824 in Mouse Visual Cortex. *Neuron* **98**, 602-615 e608, doi:10.1016/j.neuron.2018.03.037
825 (2018).
- 826 32 Fu, Y. *et al.* A cortical circuit for gain control by behavioral state. *Cell* **156**, 1139-1152,
827 doi:10.1016/j.cell.2014.01.050 (2014).
- 828 33 Kash, T. L. The role of biogenic amine signaling in the bed nucleus of the stria terminals
829 in alcohol abuse. *Alcohol* **46**, 303-308, doi:10.1016/j.alcohol.2011.12.004 (2012).
- 830 34 Yorgason, J. T., Ferris, M. J., Steffensen, S. C. & Jones, S. R. Frequency-dependent effects
831 of ethanol on dopamine release in the nucleus accumbens. *Alcohol Clin Exp Res* **38**, 438-
832 447, doi:10.1111/acer.12287 (2014).

- 833 35 Pleil, K. E. *et al.* NPY signaling inhibits extended amygdala CRF neurons to suppress binge
834 alcohol drinking. *Nat Neurosci* **18**, 545-552, doi:10.1038/nn.3972 (2015).
- 835 36 Kumar, S. *et al.* The role of GABA(A) receptors in the acute and chronic effects of ethanol:
836 a decade of progress. *Psychopharmacology (Berl)* **205**, 529-564, doi:10.1007/s00213-009-
837 1562-z (2009).
- 838 37 Woodward, J. J. & Pava, M. Ethanol inhibition of up-states in prefrontal cortical neurons
839 expressing the genetically encoded calcium indicator GCaMP3. *Alcohol Clin Exp Res* **36**,
840 780-787, doi:10.1111/j.1530-0277.2011.01674.x (2012).
- 841 38 Cheng, Y. *et al.* Distinct Synaptic Strengthening of the Striatal Direct and Indirect
842 Pathways Drives Alcohol Consumption. *Biol Psychiatry* **81**, 918-929,
843 doi:10.1016/j.biopsych.2016.05.016 (2017).
- 844 39 Badanich, K. A., Mulholland, P. J., Beckley, J. T., Trantham-Davidson, H. & Woodward,
845 J. J. Ethanol reduces neuronal excitability of lateral orbitofrontal cortex neurons via a
846 glycine receptor dependent mechanism. *Neuropsychopharmacology* **38**, 1176-1188,
847 doi:10.1038/npp.2013.12 (2013).
- 848 40 Rodriguez-Romaguera, J. *et al.* Prepronociceptin-Expressing Neurons in the Extended
849 Amygdala Encode and Promote Rapid Arousal Responses to Motivationally Salient
850 Stimuli. *Cell Rep* **33**, 108362, doi:10.1016/j.celrep.2020.108362 (2020).
- 851 41 Koob, G. F. A role for brain stress systems in addiction. *Neuron* **59**, 11-34,
852 doi:10.1016/j.neuron.2008.06.012 (2008).
- 853 42 Naegeli, C. *et al.* Locus Coeruleus Activity Mediates Hyperresponsiveness in
854 Posttraumatic Stress Disorder. *Biol Psychiatry* **83**, 254-262,
855 doi:10.1016/j.biopsych.2017.08.021 (2018).
- 856 43 Koob, G. F. Corticotropin-releasing factor, norepinephrine, and stress. *Biol Psychiatry* **46**,
857 1167-1180, doi:10.1016/s0006-3223(99)00164-x (1999).
- 858 44 Bloch, S., Rinker, J. A., Marcus, M. M. & Mulholland, P. J. Absence of effects of
859 intermittent access to alcohol on negative affective and anxiety-like behaviors in male and
860 female C57BL/6J mice. *Alcohol* **88**, 91-99, doi:10.1016/j.alcohol.2020.07.011 (2020).
- 861 45 Chen, P. *et al.* Prefrontal Cortex Corticotropin-Releasing Factor Neurons Control
862 Behavioral Style Selection under Challenging Situations. *Neuron*,
863 doi:10.1016/j.neuron.2020.01.033 (2020).
- 864 46 Arnsten, A. F., Wang, M. J. & Paspalas, C. D. Neuromodulation of thought: flexibilities
865 and vulnerabilities in prefrontal cortical network synapses. *Neuron* **76**, 223-239,
866 doi:10.1016/j.neuron.2012.08.038 (2012).
- 867 47 Arnsten, A. F. Stress signalling pathways that impair prefrontal cortex structure and
868 function. *Nat Rev Neurosci* **10**, 410-422, doi:10.1038/nrn2648 (2009).
- 869 48 Kaysen, D. *et al.* Posttraumatic stress disorder, alcohol use, and physical health concerns.
870 *J Behav Med* **31**, 115-125, doi:10.1007/s10865-007-9140-5 (2008).
- 871 49 Vazey, E. M., den Hartog, C. R. & Moorman, D. E. Central Noradrenergic Interactions
872 with Alcohol and Regulation of Alcohol-Related Behaviors. *Handb Exp Pharmacol*,
873 doi:10.1007/164_2018_108 (2018).
- 874 50 Gilpin, N. W. & Weiner, J. L. Neurobiology of comorbid post-traumatic stress disorder
875 and alcohol-use disorder. *Genes Brain Behav* **16**, 15-43, doi:10.1111/gbb.12349 (2017).
- 876 51 Halladay, L. R. *et al.* Prefrontal Regulation of Punished Ethanol Self-administration. *Biol*
877 *Psychiatry* **87**, 967-978, doi:10.1016/j.biopsych.2019.10.030 (2020).

- 878 52 Linsenbardt, D. N., Timme, N. M. & Lapish, C. C. Encoding of the Intent to Drink Alcohol
879 by the Prefrontal Cortex Is Blunted in Rats with a Family History of Excessive Drinking.
880 *eNeuro* **6**, doi:10.1523/ENEURO.0489-18.2019 (2019).
- 881 53 Linsenbardt, D. N. & Lapish, C. C. Neural Firing in the Prefrontal Cortex During Alcohol
882 Intake in Alcohol-Preferring "P" Versus Wistar Rats. *Alcohol Clin Exp Res* **39**, 1642-1653,
883 doi:10.1111/acer.12804 (2015).
- 884 54 Cannady, R., Nimitvilai-Roberts, S., Jennings, S. D., Woodward, J. J. & Mulholland, P. J.
885 Distinct Region- and Time-Dependent Functional Cortical Adaptations in C57BL/6J Mice
886 after Short and Prolonged Alcohol Drinking. *eNeuro* **7**, doi:10.1523/ENEURO.0077-
887 20.2020 (2020).
- 888 55 Siciliano, C. A. *et al.* A cortical-brainstem circuit predicts and governs compulsive alcohol
889 drinking. *Science* **366**, 1008-1012, doi:10.1126/science.aay1186 (2019).
- 890 56 Rinker, J. A. *et al.* Monitoring Neural Activity During Exposure to Drugs of Abuse With
891 In Vivo Fiber Photometry. *bioRxiv*, 487546, doi:10.1101/487546 (2018).
- 892 57 Seif, T. *et al.* Cortical activation of accumbens hyperpolarization-active NMDARs
893 mediates aversion-resistant alcohol intake. *Nat Neurosci* **16**, 1094-1100,
894 doi:10.1038/nn.3445 (2013).
- 895 58 Millan, E. Z., Kim, H. A. & Janak, P. H. Optogenetic activation of amygdala projections
896 to nucleus accumbens can arrest conditioned and unconditioned alcohol consummatory
897 behavior. *Neuroscience* **360**, 106-117, doi:10.1016/j.neuroscience.2017.07.044 (2017).
- 898 59 Zakiniaez, Y., Scheinost, D., Seo, D., Sinha, R. & Constable, R. T. Cingulate cortex
899 functional connectivity predicts future relapse in alcohol dependent individuals.
900 *Neuroimage Clin* **13**, 181-187, doi:10.1016/j.nicl.2016.10.019 (2017).
- 901 60 Cheetham, A. *et al.* Volumetric differences in the anterior cingulate cortex prospectively
902 predict alcohol-related problems in adolescence. *Psychopharmacology (Berl)* **231**, 1731-
903 1742, doi:10.1007/s00213-014-3483-8 (2014).
- 904 61 Critchley, H. D., Wiens, S., Rotshtein, P., Ohman, A. & Dolan, R. J. Neural systems
905 supporting interoceptive awareness. *Nat Neurosci* **7**, 189-195, doi:10.1038/nn1176 (2004).
- 906 62 Thiele, T. E., Crabbe, J. C. & Boehm, S. L., 2nd. "Drinking in the Dark" (DID): a simple
907 mouse model of binge-like alcohol intake. *Curr Protoc Neurosci* **68**, 9 49 41-12,
908 doi:10.1002/0471142301.ns0949s68 (2014).
- 909 63 Breton-Provencher, V. & Sur, M. Active control of arousal by a locus coeruleus
910 GABAergic circuit. *Nat Neurosci* **22**, 218-228, doi:10.1038/s41593-018-0305-z (2019).
- 911 64 Privitera, M. *et al.* A complete pupillometry toolbox for real-time monitoring of locus
912 coeruleus activity in rodents. *Nat Protoc* **15**, 2301-2320, doi:10.1038/s41596-020-0324-6
913 (2020).
- 914 65 Abernathy, K., Chandler, L. J. & Woodward, J. J. Alcohol and the prefrontal cortex. *Int*
915 *Rev Neurobiol* **91**, 289-320, doi:10.1016/S0074-7742(10)91009-X (2010).
- 916 66 Kohn, A., Coen-Cagli, R., Kanitscheider, I. & Pouget, A. Correlations and Neuronal
917 Population Information. *Annu Rev Neurosci* **39**, 237-256, doi:10.1146/annurev-neuro-
918 070815-013851 (2016).
- 919 67 Cohen, M. R. & Kohn, A. Measuring and interpreting neuronal correlations. *Nat Neurosci*
920 **14**, 811-819, doi:10.1038/nn.2842 (2011).
- 921 68 Musall, S., Kaufman, M. T., Juavinett, A. L., Gluf, S. & Churchland, A. K. Single-trial
922 neural dynamics are dominated by richly varied movements. *Nat Neurosci* **22**, 1677-1686,
923 doi:10.1038/s41593-019-0502-4 (2019).

- 924 69 Vinck, M., Batista-Brito, R., Knoblich, U. & Cardin, J. A. Arousal and locomotion make
925 distinct contributions to cortical activity patterns and visual encoding. *Neuron* **86**, 740-754,
926 doi:10.1016/j.neuron.2015.03.028 (2015).
- 927 70 Kuchibhotla, K. V. *et al.* Parallel processing by cortical inhibition enables context-
928 dependent behavior. *Nat Neurosci* **20**, 62-71, doi:10.1038/nn.4436 (2017).
- 929 71 Knoblich, U., Huang, L., Zeng, H. & Li, L. Neuronal cell-subtype specificity of neural
930 synchronization in mouse primary visual cortex. *Nat Commun* **10**, 2533,
931 doi:10.1038/s41467-019-10498-1 (2019).
- 932 72 Huda, R. *et al.* Distinct prefrontal top-down circuits differentially modulate sensorimotor
933 behavior. *Nat Commun* **11**, 6007, doi:10.1038/s41467-020-19772-z (2020).
- 934 73 O'Banion, C. P. & Yasuda, R. Fluorescent sensors for neuronal signaling. *Curr Opin*
935 *Neurobiol* **63**, 31-41, doi:10.1016/j.conb.2020.02.007 (2020).
- 936 74 O'Herron, P., Summers, P. M., Shih, A. Y., Kara, P. & Woodward, J. J. In vivo two-photon
937 imaging of neuronal and brain vascular responses in mice chronically exposed to ethanol.
938 *Alcohol* **85**, 41-47, doi:10.1016/j.alcohol.2019.12.001 (2020).
- 939 75 Ye, L. *et al.* Ethanol abolishes vigilance-dependent astroglia network activation in mice by
940 inhibiting norepinephrine release. *Nat Commun* **11**, 6157, doi:10.1038/s41467-020-19475-
941 5 (2020).
- 942 76 Juczewski, K., Koussa, J. A., Kesner, A. J., Lee, J. O. & Lovinger, D. M. Stress and
943 behavioral correlates in the head-fixed method: stress measurements, habituation
944 dynamics, locomotion, and motor-skill learning in mice. *Sci Rep* **10**, 12245,
945 doi:10.1038/s41598-020-69132-6 (2020).
- 946 77 Stowell, R. D. *et al.* Noradrenergic signaling in the wakeful state inhibits microglial
947 surveillance and synaptic plasticity in the mouse visual cortex. *Nat Neurosci*,
948 doi:10.1038/s41593-019-0514-0 (2019).
- 949 78 Jun, J. J. *et al.* Fully integrated silicon probes for high-density recording of neural activity.
950 *Nature* **551**, 232-236, doi:10.1038/nature24636 (2017).
- 951 79 Gilpin, N. W., Herman, M. A. & Roberto, M. The central amygdala as an integrative hub
952 for anxiety and alcohol use disorders. *Biol Psychiatry* **77**, 859-869,
953 doi:10.1016/j.biopsych.2014.09.008 (2015).
- 954 80 Corbit, L. H. & Janak, P. H. Habitual Alcohol Seeking: Neural Bases and Possible
955 Relations to Alcohol Use Disorders. *Alcohol Clin Exp Res* **40**, 1380-1389,
956 doi:10.1111/acer.13094 (2016).
- 957 81 Silberman, Y. *et al.* Neurobiological mechanisms contributing to alcohol-stress-anxiety
958 interactions. *Alcohol* **43**, 509-519, doi:10.1016/j.alcohol.2009.01.002 (2009).
- 959 82 Becker, H. C., Lopez, M. F. & Doremus-Fitzwater, T. L. Effects of stress on alcohol
960 drinking: a review of animal studies. *Psychopharmacology (Berl)* **218**, 131-156,
961 doi:10.1007/s00213-011-2443-9 (2011).
- 962 83 Hopf, F. W. & Lesscher, H. M. Rodent models for compulsive alcohol intake. *Alcohol* **48**,
963 253-264, doi:10.1016/j.alcohol.2014.03.001 (2014).
- 964 84 Vendruscolo, L. F. *et al.* Corticosteroid-dependent plasticity mediates compulsive alcohol
965 drinking in rats. *J Neurosci* **32**, 7563-7571, doi:10.1523/JNEUROSCI.0069-12.2012
966 (2012).
- 967 85 Hangya, B., Ranade, S. P., Lorenc, M. & Kepecs, A. Central Cholinergic Neurons Are
968 Rapidly Recruited by Reinforcement Feedback. *Cell* **162**, 1155-1168,
969 doi:10.1016/j.cell.2015.07.057 (2015).

- 970 86 Janssen, P. & Shadlen, M. N. A representation of the hazard rate of elapsed time in
971 macaque area LIP. *Nat Neurosci* **8**, 234-241, doi:10.1038/nn1386 (2005).
- 972 87 Seiler, J. L., Cosme, C. V., Sherathiya, V. N., Bianco, J. M. & Lerner, T. N. Dopamine
973 Signaling in the Dorsomedial Striatum Promotes Compulsive Behavior. *bioRxiv*,
974 2020.2003.2030.016238, doi:10.1101/2020.03.30.016238 (2020).
- 975 88 Tu, Y. *et al.* Ethanol inhibits persistent activity in prefrontal cortical neurons. *J Neurosci*
976 **27**, 4765-4775, doi:10.1523/JNEUROSCI.5378-06.2007 (2007).
- 977 89 Morningstar, M. D., Linsenbardt, D. N. & Lapish, C. C. Ethanol Alters Variability, But
978 Not Rate, of Firing in Medial Prefrontal Cortex Neurons of Awake-Behaving Rats. *Alcohol*
979 *Clin Exp Res* **44**, 2225-2238, doi:10.1111/acer.14463 (2020).
- 980 90 Khan, A. G. *et al.* Distinct learning-induced changes in stimulus selectivity and interactions
981 of GABAergic interneuron classes in visual cortex. *Nat Neurosci* **21**, 851-859,
982 doi:10.1038/s41593-018-0143-z (2018).
- 983 91 Cardin, J. A. Inhibitory Interneurons Regulate Temporal Precision and Correlations in
984 Cortical Circuits. *Trends Neurosci* **41**, 689-700, doi:10.1016/j.tins.2018.07.015 (2018).
- 985 92 Lee, S., Kruglikov, I., Huang, Z. J., Fishell, G. & Rudy, B. A disinhibitory circuit mediates
986 motor integration in the somatosensory cortex. *Nat Neurosci* **16**, 1662-1670,
987 doi:10.1038/nn.3544 (2013).
- 988 93 Pi, H. J. *et al.* Cortical interneurons that specialize in disinhibitory control. *Nature* **503**,
989 521-524, doi:10.1038/nature12676 (2013).
- 990 94 Pfeffer, C. K., Xue, M., He, M., Huang, Z. J. & Scanziani, M. Inhibition of inhibition in
991 visual cortex: the logic of connections between molecularly distinct interneurons. *Nat*
992 *Neurosci* **16**, 1068-1076, doi:10.1038/nn.3446 (2013).
- 993 95 Centanni, S. W., Burnett, E. J., Trantham-Davidson, H. & Chandler, L. J. Loss of delta-
994 GABAA receptor-mediated tonic currents in the adult prelimbic cortex following
995 adolescent alcohol exposure. *Addict Biol* **22**, 616-628, doi:10.1111/adb.12353 (2017).
- 996 96 Pleil, K. E. *et al.* Effects of chronic ethanol exposure on neuronal function in the prefrontal
997 cortex and extended amygdala. *Neuropharmacology* **99**, 735-749,
998 doi:10.1016/j.neuropharm.2015.06.017 (2015).
- 999 97 Dao, N. C., Brockway, D. F., Nair, M. S. & Crowley, N. A. Bi-directional control of a
1000 prelimbic somatostatin microcircuit decreases binge alcohol consumption. *bioRxiv*,
1001 2020.2011.2027.400465, doi:10.1101/2020.11.27.400465 (2020).
- 1002 98 Joffe, M. E., Winder, D. G. & Conn, P. J. Contrasting sex-dependent adaptations to
1003 synaptic physiology and membrane properties of prefrontal cortex interneuron subtypes in
1004 a mouse model of binge drinking. *Neuropharmacology* **178**, 108126,
1005 doi:10.1016/j.neuropharm.2020.108126 (2020).
- 1006 99 Nimitvilai, S., Lopez, M. F. & Woodward, J. J. Effects of monoamines on the intrinsic
1007 excitability of lateral orbitofrontal cortex neurons in alcohol-dependent and non-dependent
1008 female mice. *Neuropharmacology* **137**, 1-12, doi:10.1016/j.neuropharm.2018.04.019
1009 (2018).
- 1010 100 Aston-Jones, G., Foote, S. L. & Bloom, F. E. Low doses of ethanol disrupt sensory
1011 responses of brain noradrenergic neurones. *Nature* **296**, 857-860, doi:10.1038/296857a0
1012 (1982).
- 1013 101 Berridge, C. W. Noradrenergic modulation of arousal. *Brain Res Rev* **58**, 1-17,
1014 doi:10.1016/j.brainresrev.2007.10.013 (2008).

- 1015 102 Kashem, M. A. *et al.* Actions of alcohol in brain: Genetics, Metabolomics, GABA
1016 receptors, Proteomics and Glutamate Transporter GLAST/EAAT1. *Curr Mol Pharmacol*,
1017 doi:10.2174/1874467213666200424155244 (2020).
- 1018 103 Harrison, N. L. *et al.* Effects of acute alcohol on excitability in the CNS.
1019 *Neuropharmacology* **122**, 36-45, doi:10.1016/j.neuropharm.2017.04.007 (2017).
- 1020 104 Gutman, A. L. & Taha, S. A. Acute ethanol effects on neural encoding of reward size and
1021 delay in the nucleus accumbens. *J Neurophysiol* **116**, 1175-1188,
1022 doi:10.1152/jn.00204.2014 (2016).
- 1023 105 Xu, M. & Woodward, J. J. Ethanol inhibition of NMDA receptors under conditions of
1024 altered protein kinase A activity. *J Neurochem* **96**, 1760-1767, doi:10.1111/j.1471-
1025 4159.2006.03703.x (2006).
- 1026 106 Adermark, L. & Lovinger, D. M. Ethanol effects on electrophysiological properties of
1027 astrocytes in striatal brain slices. *Neuropharmacology* **51**, 1099-1108,
1028 doi:10.1016/j.neuropharm.2006.05.035 (2006).
- 1029 107 Crews, F. T., Morrow, A. L., Criswell, H. & Breese, G. Effects of ethanol on ion channels.
1030 *Int Rev Neurobiol* **39**, 283-367, doi:10.1016/s0074-7742(08)60670-4 (1996).
- 1031 108 Avchalumov, Y. *et al.* Chronic ethanol exposure differentially alters neuronal function in
1032 the medial prefrontal cortex and dentate gyrus. *Neuropharmacology*, 108438,
1033 doi:10.1016/j.neuropharm.2020.108438 (2020).
- 1034 109 Pati, D. *et al.* Chronic intermittent ethanol exposure dysregulates a GABAergic
1035 microcircuit in the bed nucleus of the stria terminalis. *Neuropharmacology*, 107759,
1036 doi:10.1016/j.neuropharm.2019.107759 (2019).
- 1037 110 Renteria, R., Cazares, C. & Gremel, C. M. Habitual Ethanol Seeking and Licking
1038 Microstructure of Enhanced Ethanol Self-Administration in Ethanol-Dependent Mice.
1039 *Alcohol Clin Exp Res* **44**, 880-891, doi:10.1111/acer.14302 (2020).
- 1040 111 Pachitariu, M. *et al.* Suite2p: beyond 10,000 neurons with standard two-photon
1041 microscopy. *Biorxiv* (2017).
- 1042 112 Chen, T.-W. *et al.* Ultrasensitive fluorescent proteins for imaging neuronal activity. *Nature*
1043 **499**, 295, doi:10.1038/nature12354 (2013).